The Dissertation Committee for Li Jiang
certifies that this is the approved version of the following dissertation:

Investigation on the Holographic Principle

Committee:

Willy Fischler, Supervisor

Jacques Distler

Daniel Freed

George Sudarshan

Steven Weinberg

Investigation on the Holographic Principle

by

Li Jiang, B.S.

DISSERTATION

Presented to the Faculty of the Graduate School of

The University of Texas at Austin

in Partial Fulfillment

of the Requirements

for the Degree of

DOCTOR OF PHILOSOPHY

THE UNIVERSITY OF TEXAS AT AUSTIN

May 2003

Dedicated to my parents.

Acknowledgments

I have benefited from fruitful collaborations with Eric Nicholson and Amit Apte. I thank Prof. Willy Fischler for suggesting the research problem which led to the work done in Chapter 2. Helpful discussions on the AdS/CFT correspondence with Elie Gorbatov and Frederic Zamora are gratefully acknowledged. I also appreciate Profs. Willy Fischler and Jacques Distler's references which helped me attend the TASI 2001 Summer School. During my years at UT, I have particularly enjoyed the classes taught by Profs. Vadim Kaplunovsky, Dan Freed and Karen Uhlenbeck.

I also thank Jan Duffy, Terry Riley and Alyce Wilson for various administrative helps.

Investigation on the Holographic Principle

Publication No. ________________

Li Jiang, Ph.D.
The University of Texas at Austin, 2003

Supervisor: Willy Fischler

The holographic principle asserts that any given codimension two spacelike surface limits the information content of adjacent regions. We first review various entropy bounds which lead to the formulation of this conjecture, putting great emphasis on the UV-IR connection. We propose to use noncommutative field theory as a toy model to study the holographic mapping mechanism. In particular, we investigate how the fundamental dipole structure emerges in noncommutative gauge theories by using matrix formulation. The momentum dependent growing behavior of the dipoles can provide a simple way to map the bulk degrees of freedom onto the boundary. In the context of the AdS/CFT correspondence, which is the best known example of a holographic theory, we study the thermodynamics of $\mathcal{N} = 4$ supersymmetric Yang-Mills theory at two-loop level and compare the result to the supergravity calculation. This provides an excellent example to illustrate the idea of strong/weak duality. Questions about a possible large N phase transition still remain unsolved.

Table of Contents

List of Tables

List of Figures

Chapter 1

Holographic Principle

1.1 UV-IR Connection

In the quest for a unified description of all the fundamental interactions, gravity continues to resist joining up with the other three forces. One basic reason is that while all the other interactions are formulated as local quantum field theory (LQFT), gravity is essentially nonlocal. This peculiar feature of gravity can be understood from black hole physics. LQFT is based on quantum mechanics and special relativity. One of the fundamental principles of quantum mechanics is the Heisenberg uncertainty relation, according to which, the more momentum one deposits locally, the shorter distance one can probe. This is certainly true in the absence of gravity. However when the gravitational effect becomes important, there emerges an absolute limit on the smallest scale one can hope to resolve. The reason is that with high enough energy stored in a local region, one creates a black hole instead of digging further into shorter distance. We can formulate this statement in a mathematically precise way. As is well known, the mass of a Schwarzschild black hole is proportional to its radius $r_{\rm bh} = 2GM$, where Newton's constant can be translated into a length scale $G = \ell_{\rm p}^2$ (in D-dimensional spacetime, $G = \ell_{\rm p}^{D-2}$). By the uncertainty principle, the smallest length scale associated with M is $d = 1/M$. Combining the black hole formula with this minimum uncertainty relation, we get

$$r_{\mathrm{bh}} d = 2\ell_{\mathrm{p}}^2. \tag{1.1}$$

Since the event horizon hides all the information inside the black hole, it forbids further exploration on scale smaller than the black hole radius, *i.e.*, $d \geq 2r_{\mathrm{bh}}$. Then Eq. (1.1) gives

$$d \geq 2\ell_{\mathrm{p}}, \tag{1.2}$$

hence we see Planck length ℓ_{p} sets the absolute limit on our ability to study the microscopic world. This suggests a picture of the spacetime consisting of discrete Planck lattice at the fundamental level. However, the important point one has to realize is that the lattice is not fixed, but can grow with increasing energy. This is the so-called UV-IR connection. Eq. (1.1) can be rewritten as

$$\frac{r_{\mathrm{bh}}}{\ell_{\mathrm{p}}} = 2\frac{M}{M_{\mathrm{p}}}.$$

When $M \ll M_{\mathrm{p}}$, the black hole is so minuscule that a local observer can not detect its existence. So in such low energy range, LQFT constitutes a good description of nature. But if the typical energy scale is above M_{p} (*i.e.*, UV), the shortest distance one can resolve actually grows in accordance with the above equation (*i.e.*, IR). The physically accessible region in the phase diagram is illustrated in Fig. 1.1(a).

The UV-IR connection as discussed above only applies to a local region, for instance, in high energy scattering experiments (black hole production in TeV gravity scenario is essentially based on this relation [1]). If one attempts to excite high energy modes everywhere in a finite system, it would undergo gravitational collapse way before one reaches the Planck energy $M_{\rm p}$. This phenomenon is related to the black hole entropy and various entropy bounds, ultimately to the holographic principle (for recent reviews, see [2]). To understand this *global* UV-IR connection (as compared to the *local* one), we take a finite system of size L. Suppose the system is dominated by short distance fluctuation with wavelength $d = 1/E$, then it is effectively discretized into cells of size d. The total energy stored in the system is therefore on the order of $M = (L/d)^3 E = L^3 E^4$. In order to be gravitationally stable, M must be less than the mass of a Schwarzschild black hole with the same radius, *i.e.*, $M \leq L/4G$. This sets the upper bound on the fluctuation energy $E \leq 1/\sqrt{2\ell_{\rm p} L}$. On the other hand, the geometrical size L gives rise to an infrared cutoff since no fluctuation can be larger than the system itself. Therefore, we have

$$\frac{1}{L} \leq E \leq \frac{1}{\sqrt{2\ell_{\rm p} L}}. \tag{1.3}$$

Fig. 1.1(b) shows this version of the UV-IR relation. Note that Eq. (1.3) implies Eq. (1.2). Since a typical physical size is much larger than the Planck length, we see that $E \ll M_{\rm p}$. This improved upper energy bound (from $1/\ell_{\rm p}$ down to $1/\sqrt{2\ell_{\rm p} L}$) seems to conform to the popular view that there should be new physics other than the standard model between TeV and the Planck scale. If one equates $1/\sqrt{2\ell_{\rm p} L}$ with 1 TeV, L turns out to be 0.12 cm, which is large enough to accommodate any typical scattering process (cross section is measured in 1 barn $= 10^{-24}$cm^2). We find this millimeter

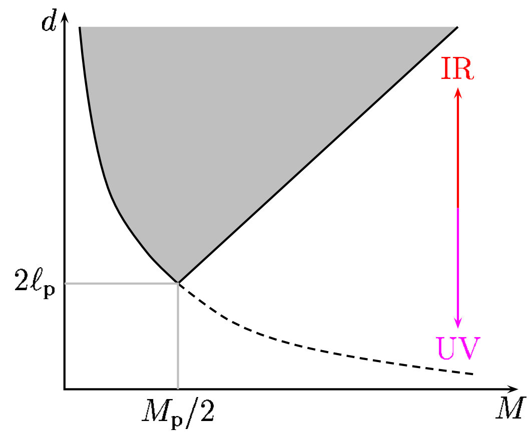

(a) Local UV-IR

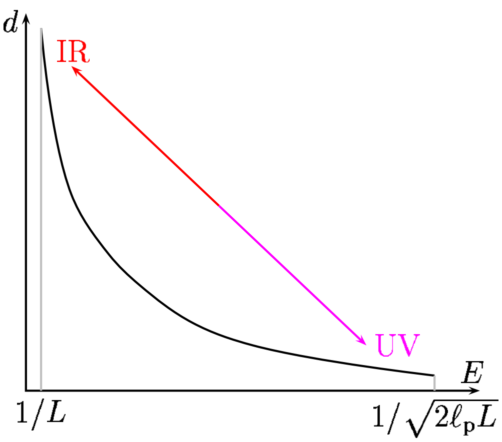

(b) Global UV-IR

Figure 1.1: The UV-IR connection is represented in two different ways: (a) combines the uncertainty principle with black hole physics and shows the physically accessible region as the shaded area; (b) is based on the global consideration and implies the same absolute minimum length scale as in (a).

scale from TeV very interesting, especially in view of the fact that millimeter size extra dimensions arise from a TeV fundamental Planck scale in the large extra dimension scenario [3]. In fact, $E_{\rm UV} = 1/\sqrt{2\ell_{\rm p} L}$ happens to be the same as $M_{\rm p} = M^2 R$ in the case of two extra dimensions (where M is the fundamental gravity scale and R is the size of the extra dimensions). Whether this similarity is a coincidence or not remains unclear to us. But it seems unlikely this identification of $E_{\rm UV}$ with TeV would solve the hierarchy problem. For one thing, supersymmetric theories, the most promising extension of the standard model beyond TeV, are local. This suggests LQFT may still work above the TeV scale.

These two versions of the UV-IR connection have been recognized for a long time (see, for instance, [2], for further discussion).[1] Here we present a third form of the UV-IR mixing, which is derived from black hole thermodynamics. Black holes, as thermodynamical entities, have a temperature. Unlike the ordinary systems, this temperature is directly related to the black hole radius ($T = 1/4\pi r_{\rm bh}$ for a Schwarzschild black hole). From the definition of the partition function for a thermodynamical system, $Z = \sum e^{-\beta E}$, we see that temperature acts as a kind of UV cutoff. All the states with energy E above temperature T are exponentially suppressed due to the Boltzmann factor. The higher the temperature, the shorter the thermal wavelength (for massless modes, $\lambda_{\rm th} \sim 1/T$), so temperature dictates how large a local probe can be. Clearly, this local probe has nothing to do with the macroscopic size

[1] Although the terminology of local *versus* global is new here.

of the system based on our intuition from LQFT. But for black holes, this is not true, UV (temperature) and IR (geometric size) are intimately related to each other. Since temperature labels the energy density of the system,[2] this form of UV-IR mixing is close to the global version discussed before.

If we want to build a model of gravity in an attempt to capture some of its nonlocal features, this model must manifest the UV-IR connection in some way. Noncommutative field theory (NCFT) seems to be a good candidate to start with. Formally, NCFT can be regarded as the effective description of the worldvolume of D-branes in the background of Neveu-Schwarz (NS) B field in the decoupling limit in string theory [4]. The noncommutativity parameter θ is related to B via $\theta = 1/B$. Since $B_{\mu\nu}$ and the graviton $g_{\mu\nu}$ are different decomposition of $\mathbf{8_v} \times \mathbf{8_v}$ in the NS-NS sector, it does not come as a surprise that NCFT may behave in a way similar to gravity. In order to make this analogy more concrete, we summarize two characteristics of gravity: first, there is a dimensional constant G (or written in the form of $\ell_{\rm p}$ or $M_{\rm p}$), which is spelled out in Eq. (1.1); second, the UV-IR connection embodies all the nonlocal features through three different (yet related) forms as presented earlier. The defining property of NCFT is that coordinates do not commute

$$[x^\mu, x^\nu] = i\theta^{\mu\nu}, \tag{1.4}$$

from which one can infer a minimum uncertainty relation $\Delta x \Delta y \sim \theta$ similar to Eq. (1.1). So $\sqrt{\theta}$ plays the role of Planck length $\ell_{\rm p}$. In fact, it has been

[2]This is so even for a Schwarzschild black hole, $\rho \sim T^2/G$, although it has negative specific heat.

shown the effective quanta of NCFT are dipoles with transverse size growing with their center of mass momentum, $x^\mu = \theta^{\mu\nu} p_\nu$ [5]. The explicit dipole structure of noncommutative gauge theories in terms of Wilson line operators was shown in [6] by using matrix formulation, this will be the subject of Chapter 3. This momentum dependent growing behavior resembles that of black holes, though unlike black holes, a dipole does not grow in volume. It has also been discovered by perturbative analysis that NCFT has UV-IR mixing: high energy modes running around loop in Feynman diagrams produce singular behavior in the external momenta [7]. This actually explains why low energy effective theory of NCFT exhibits long distance interactions. Thus NCFT possess both peculiarities of gravity, though not in completely identical form. This raises the hope that we may gain some knowledge of gravity in the relatively simpler framework of NCFT.

1.2 Holographic Mapping

Holographic principle, loosely speaking, asserts that any given codimension two spacelike surface limits the information content of adjacent regions. However, the principle itself does not give any clue as to how the bulk degrees of freedom are mapped onto the holographic screen. This is one major motivation to model gravity using NCFT. As will be explained later, growing dipoles provide a simple mapping mechanism to encode the information.

It is helpful to first review various entropy bounds which lead to the formulation of the holographic principle. Early studies of black hole reveal that it is only characterized by its mass, angular momentum and charge. This discovery poses a problem: if a matter system undergoes gravitational collapse and converts into a black hole, the entropy associated with the original system seems to disappear since the final state is unique. This process clearly violates the second law of thermodynamics. By noting another result of black hole physics, namely its horizon area A never decreases, Bekenstein [8] proposed that a black hole carries an entropy proportional to its horizon area and that the total entropy of ordinary matter system and black hole never decreases, hence the generalized second law (GSL). The idea that a black hole behaves like a thermodynamical entity is substantiated by Hawking's discovery of black hole radiation [9], and this leads to the now well known entropy formula[3]

$$S_{\mathrm{bh}} = \frac{A}{4}. \tag{1.5}$$

Now consider an ordinary matter system of energy E and size R (R is the radius of the smallest sphere circumscribing the system). If we drop this system into a large black hole (the so-called Geroch process) and demand that GSL holds, the lost matter entropy must be compensated by the black hole entropy increase $S_{\mathrm{matter}} \leq \delta S_{\mathrm{bh}}$. This gives rise to the *Bekenstein bound* [10] on the matter entropy

$$S_{\mathrm{matter}} \leq 2\pi E R. \tag{1.6}$$

Another way to obtain an upper bound is via the Susskind process, which basically says that a black hole is the end product of mass aggregation. There

[3]The area A is measured in units of ℓ_{p}^2.

are some assumptions involved such as spherically symmetric and weakly gravitating. The initial matter entropy has to be less or equal to the final black hole entropy by GSL

$$S_{\text{matter}} \leq \frac{A}{4}. \tag{1.7}$$

This *spherical entropy bound* is actually weaker than the Bekenstein bound because a gravitationally stable system (ordinary matter) satisfies $E \leq R/2$ and the horizon area $A = 4\pi R^2$. But it admits easier generalization to broader cases. By dropping the assumption of asymptotic structure, spherical symmetry and gravitational stability, one is led to the *spacelike entropy bound*

$$S(V) \leq \frac{A[B(V)]}{4} \tag{1.8}$$

where V is any compact spatial region and $B(V)$ is its boundary.

Motivated by these entropy bounds, 't Hooft, and later, Susskind [11] proposed that not only the entropy, but all the fundamental degrees of freedom within a region are bounded by its boundary area. This radical proposal is much stronger than the original entropy bound because entropy is always less than the number of total degrees of freedom $S < N$ [4] and it is not obvious at all that Eq. (1.8) implies

$$N(V) \leq \frac{A[B(V)]}{4}. \tag{1.9}$$

Unitarity and UV-IR connection played crucial roles in the argument. Consider an ordinary system of volume V which evolves into a black hole. LQFT tells us

[4] The number of total degrees of freedom of a system is defined as the logarithm of the dimension of its Hilbert space $N = \ln[\dim\mathcal{H}]$.

the initial Hilbert space has dimension $\dim\mathcal{H} \sim e^V$; but for the final black hole $\dim\mathcal{H} = e^{A/4}$ because $N_{\rm bh} = S_{\rm bh}$ by the UV-IR connection (the entropy of an ordinary system increases with temperature, but it is fixed by the geometric size of a black hole). If the quantum evolution is unitary for this process, the Hilbert space must have the same dimension $e^{A/4}$ throughout. In fact, measured in units of $\ell_{\rm p}^3$, e^V significantly overestimates the number of degrees of freedom since LQFT has already broken down at such high energy as discussed in the previous section.

All these ideas are astonishing and interesting except that the entropy bound itself is not valid in general, so the holographic principle as originally presented is on a shaky ground. The spacelike entropy bound Eq. (1.8) can be violated in a number of ways such as when applied to nontrivial topology, gravitational collapse and certain types of cosmology (see [2] for a detailed analysis). Because of the difficulties with spacelike entropy bound, Fischler and Susskind employed a light cone construction to show that the bound still holds within the particle horizon in flat and open Friedmann-Robertson-Walker (FRW) universes [12]. This valid region was subsequently generalized to within the Hubble horizon [13] and the apparent horizon [14], but all of them have some limitations. The light cone approach was extended by Bousso, who discovered a universal covariant formulation of the entropy bound [15].

The key concept in Bousso's construction is the *light-sheet*. For the sake of simplicity, we assume spherical symmetry in the following discussion. Given any codimension two spatial surface B, there are four null hypersurfaces emanating from it. If the area A of spatial slicing along some null direction does not increase away from B, $\theta(\lambda) \equiv \frac{dA}{d\lambda}/A \leq 0$ (λ is the affine parameter along the light ray), that null hypersurface is called a light-sheet $L(B)$. It is easy to see there are at least two light-sheets associated with every B since out of a pair of opposite null directions at most only one is expanding. By construction, light-sheets terminate at caustics, *i.e.*, when light rays start to expand. The *covariant entropy bound* states that the entropy across each light-sheet is bounded by one quarter the area of B:

$$S[L(B)] \leq \frac{A(B)}{4}. \tag{1.10}$$

One important difference between the covariant entropy bound and all the previous results is that the new approach starts with a surface and then select the right region via light-sheets, exactly in the opposite order of the traditional methods. A general spacetime can be divided into several different regions: *normal* (weak gravity), *trapped* (such as inside the black hole horizon or near the big crunch) and *anti-trapped* (such as near the big bang). The boundary between the normal and (anti-)trapped regions is called apparent horizon,[5] where the expansion of light rays vanishes $\theta = 0$. Within different regions, light-sheets orients in different directions. For instance, near the big bang there are two past directed light-sheets. Therefore, depending on where the spacelike surface B resides in spacetime, the relevant region whose information content is limited by $A(B)/4$ is uniquely determined by the light-sheets. Another point

[5]For a Schwarzschild black hole, the apparent horizon coincides with its event horizon.

is that light-sheets can be truncated by the presence of spacetime singularities, hence only probe the vicinity of a spatial surface. From an operational point of view, we think this can be regarded as evidence for dimensional reduction in strong gravity (or at high energy). This has been used to explain why the spacelike entropy bound fails for a collapsing star. In fact, the spacelike entropy bound is a special case of the covariant one when B is a closed surface and $L(B)$ is complete (light rays form a cone) [15]. Bousso has shown the validity of the covariant entropy bound in an extremely broad range of examples [2].

Now we have a generally valid entropy bound,[6] how is it related to the holographic principle? Since the covariant entropy bound is symmetric under time reversal, it can not be originated thermodynamically. This strongly suggests it has to be a bound on all the degrees of freedom in nature and therefore reinforce the original holographic principle as a fundamental law. Again using the light-sheet formulation, Bousso gave a recipe to construct holographic screen in general spacetimes where the bulk information can be stored [19]. It is clear that a stack of (past) light cones along any worldline foliates the spacetime. Following the light cone emanating at time t, its spatial area will either increase indefinitely as in anti-de Sitter (AdS) space or reaches a maximum and then decreases as in FRW universe. In the former case, the

[6]Up to now we have barely mentioned quantum effects in the geometry. Lowe [16] argued the covariant entropy bound could be violated when taking Hawking radiation into account. However, it was rebuffed by Bousso [17]. Very recently, Strominger and Thompson [18] proposed to add the quantum entanglement entropy across the surface to its area, and asserted that the total should surpass the matter entropy. This very important yet unsettled issue calls for further investigation.

conformal boundary $\mathcal{B}$ of the spacetime will encode all the information on the light cone since it is a light-sheet by definition; in the latter, the maximum surface $B(t)$ divides the light cone into two parts, both are light-sheets again since away from $B(t)$ the expansion is non-positive. Applying the covariant entropy bound to each light-sheet separately and adding them up, we find that the information on the whole light cone is bounded by

$$N(t) \leq \frac{A[B(t)]}{2}. \tag{1.11}$$

For each light cone, there is a $B(t)$. This sequence of surfaces form a codimension one hypersurface, which is exactly the apparent horizon $\mathcal{A}$ if we recall the expansion of light rays θ flips sign across $\mathcal{A}$. In conclusion, all the fundamental degrees of freedom in the entire spacetime can be encoded on either its conformal boundary $\mathcal{B}$ or the apparent horizon $\mathcal{A}$ or a combination of the two. And the holographic screen can be called $\mathcal{AB}$-screen.[7]

The construction of holographic screen is straightforward, but the question about the mapping mechanism still remains. Tremendous efforts have been devoted to find an explanation of the black hole entropy Eq. (1.5). Most studies focus on the horizon itself: if some effective degrees of freedom can be identified on the horizon, the corresponding entropy will certainly scale like its area. Of course it is nontrivial to sort out these effective modes and check the 1/4 coefficient. But it is not clear how the bulk degrees of freedom are mapped onto the horizon. For instance, consider a physical process where gravitational

[7] We coined this term.

effect gradually becomes strong and eventually turns the system into a black hole. We want to know more about the transition from the initial local bulk description to the final effective boundary theory. It is this transition that was poorly understood in the literature. In fact, an even deeper question is what mechanism underlies the holographic principle. Based on the discussion presented in Section 1.1, we propose to use NCFT to model the transition from the bulk to the boundary and hope it will illustrate how the information is encoded holographically.

Consider a box of thermal noncommutative particles (described by a scalar field living on a noncommutative plane); as explained before, we really should think them as dipoles. However, at low temperature, these dipoles are very small in extension and there is virtually no distinction from the particles, so we expect their thermodynamical properties to be the same as that of a conventional system, *i.e.*, described by LQFT. When temperature rises, more high energy modes are excited, hence dipoles grow with increasing momenta. As a result, their macroscopic properties start to deviate from the particle gas. Put it another way, higher temperature means shorter thermal wavelength. When $\lambda_{\rm th}$ is short enough to detect the existence of a fundamental length scale $\sqrt{\theta}$, the differences between dipole and particle gases become prominent. Eventually, dipoles can grow as big as the box itself but no bigger. At this point, temperature seems to reach a maximum L/θ, where L is the size of the system (recall the relation $x^\mu = \theta^{\mu\nu} p_\nu$ if one identifies the momentum with temperature). One can understand this by noting that the corresponding

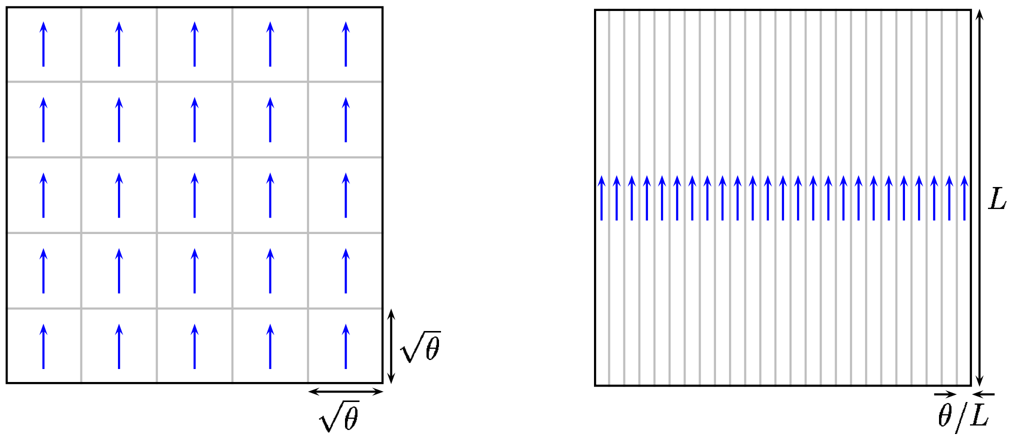

(a) Lattice at low temperature (b) Lattice at high temperature

Figure 1.2: Ising model on a noncommutative plane: when the thermal wavelength is comparable to $\sqrt{\theta}$, dipoles show up with one spin per cell (denoted by a blue arrow); at high temperature L/θ, they grow long enough to touch the boundaries of the box, hence the 2-D model degenerates into a chain and the bulk information is completely encoded on the boundary.

thermal wavelength $\lambda_{\text{th}} = \theta/L$ is the smallest scale one can get for this system. This is in contrast with any conventional systems, in which temperature can in principle rises to infinity. Thus the UV-IR mixing characteristic of NCFT magically connects temperature to the system size just like in the black hole case. Essentially we are dealing with an incompressible fluid consisting of unit cells of area θ. The holographic mapping can be easily understood in the following way. As shown in Fig. 1.2 is a box with 25 cells in it, each cell (dipole) carries a spin or some other internal degrees of freedom. When the box is boosted along the horizontal axis, all the dipoles stretch out in the orthogonal direction, spanning across the entire box at high enough energy (this simulates high temperature situation). Because of incompressibility, the total number of cells stay the same. Then as temperature increases this two-dimensional Ising model effectively reduces to one dimension. By collecting the data on its boundary, we know all the information inside the box. Here the growing dipoles provide a mapping mechanism from the bulk onto its boundary. This simple picture suggests that holography manifests itself only at high energy. At low energy, LQFT is good enough (represented here by the 2-D Ising model); but when gravity is strong, a boundary (or screen in general) description is then preferred. The point is that in the low energy region, physically accessible degrees of freedom are always finite regardless of how large the fundamental set is, a complete holographic theory is redundant and hard to construct since one has to extract a finite subset out of the complete information. Dimensionally reduced description at high energy seems to agree with Bousso's covariant formulation, where light-sheets are often truncated in strong gravity and only probe the vicinity of a spatial surface.

It will be more convincing if we can carry out an explicit calculation which shows all the features we discussed above. However, there are some technical difficulties with a finite system on noncommutative plane, we defer the discussion to Chapter 3.

1.3 AdS/CFT Correspondence

At present, the AdS/CFT correspondence [20] is the best known example of a holographic theory, which states that type IIB string theory on $AdS_5 \times S^5$ background is equivalent to $\mathcal{N} = 4$ $SU(N)$ supersymmetric Yang-

Mills (SYM) theory on its boundary (for reviews, see [21]). On the string side, both AdS_5 and S^5 have identical radius $L^4 = 4\pi g_s N \alpha'^2$, where N is the flux of the five-form Ramond-Ramond (R-R) field through S^5; on the field theory side, the available parameters are the gauge coupling $g_{\rm YM}$ and the number of colors N. These two sets of parameters are related by[8]

$$4\pi g_s = g_{\rm YM}^2. \tag{1.12}$$

Both sides admit a perturbative double expansion: string calculation can be organized into loop correction (in g_s) and string modes correction (in α'); while Feynman diagrams in gauge theory can be classified by their topology (N^{2-2g}, where g is the genus of the surface) and the power of the 't Hooft coupling $\lambda = g_{\rm YM}^2 N$. Correspondingly, there are two limits we can take. In field theory, if λ is fixed while taking $N \to \infty$, the planar diagram will dominate. This is reflected by the vanishing of quantum effects in string theory. If further $\lambda \to \infty$, all the higher string modes will decouple and the classical string theory will be reduced to type IIB supergravity. So strongly coupled SYM theory is mapped onto the low energy effective theory of the string and it opens the possibility to study nonperturbative dynamics of gauge theory via gravity approach. The converse is also true, therefore we see that the strong regime on one side is dual to the weak regime on the other. These different forms of the AdS/CFT correspondence can be summarized as [21]

[8]More elegantly, we have the complex coupling $\tau \equiv \frac{\theta}{2\pi} + \frac{4\pi i}{g_{\rm YM}^2} = \frac{\chi}{2\pi} + \frac{i}{g_s}$, where the instanton angle θ is related to the expectation value of the R-R scalar χ.

	Boundary of AdS_5	$AdS_5 \times S^5$
Strong Form	$\mathcal{N} = 4$ $SU(N)$ SYM (all N and g_{YM})	full type IIB string theory (all g_{s} and α')
't Hooft Limit	$N \to \infty$ and λ fixed ($1/N$ expansion)	classical type IIB string theory (g_{s} expansion)
Weak Form	$N \to \infty$ and $\lambda \to \infty$ ($\lambda^{-1/2}$ expansion)	classical type IIB supergravity (α' expansion)

Table 1.1: The three forms of the AdS/CFT correspondence.

Gravity lives in the AdS bulk and gauge theory on its boundary. According to the correspondence, these two descriptions are exactly the same, the superconformal theory encodes all the dynamics in the interior. So it is justified to call the boundary of AdS a holographic screen. In fact as Bousso pointed out [19]: AdS space is very special, its conformal boundary forms a timelike hypersurface of constant spatial area on which complete data about the interior is encoded. We briefly review how to construct the holographic screen in AdS space using the general method outlined in Section 1.2.

AdS space is the maximally symmetric solution of the vacuum Einstein equation with a negative cosmological constant. It can be viewed as a hyperboloid in the one-dimension higher flat space (see Fig. 1.3(a)). In the embedding coordinates, AdS_5 can be expressed as

$$X_0^2 + X_5^2 - \sum_{i=1}^{4} X_i^2 = L^2, \tag{1.13}$$

and has the isometry $SO(2,4)$ by construction. This isometry is translated into the conformal symmetry in four dimensions on the field theory side. In

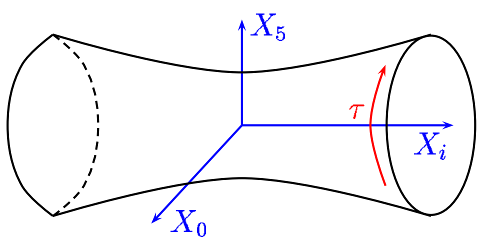

(a) Hyperboloid

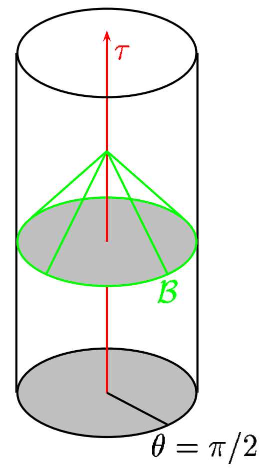

(b) $\mathbb{R} \times D^4$

Figure 1.3: AdS_5 and its conformal structure: (a) shows AdS_5 as a hyperboloid in $\mathbb{R}^{2,4}$; (b) is the corresponding Penrose diagram, where the past light cone intersects the conformal boundary $\mathcal{B}$ at $\theta = \pi/2$. The global time is denoted by τ, which is S^1 in (a) and $\mathbb{R}$ in (b).

addition, the $SO(6)$ of S^5 is related to the R-symmetry which rotates the six scalars and the four fermions in $\mathcal{N} = 4$ SYM theory. Although the S^5 does not play a role in the present discussion. Re-parameterizing the embedding coordinates $X_0 = L \cosh\rho \cos\tau$, $X_5 = L \cosh\rho \sin\tau$ and $X_i = L \sinh\rho\, \Omega_i$ ($i = 1, \cdots, 4$ and $\Omega_i \in S^3$), we find the metric on AdS_5:

$$ds^2 = L^2 \left(-\cosh^2\rho\, d\tau^2 + d\rho^2 + \sinh^2\rho\, d\Omega_3^2\right) \tag{1.14}$$

where the global time $0 \le \tau < 2\pi$ and the radial coordinate $\rho \ge 0$. To avoid the closed timelike curves, we usually consider the universal covering space of AdS, where τ is extended to $\mathbb{R}$. The conformal structure of AdS_5 can be obtained by a simple transformation $\tan\theta = \sinh\rho$ $(0 \le \theta \le \pi/2)$. Apart from an overall factor $L^2/\cos^2\theta$, Eq. (1.14) becomes

$$ds^2 = -d\tau^2 + d\theta^2 + \sin^2\theta\, d\Omega_3^2. \tag{1.15}$$

It is clear now that AdS_5 has the topology of $\mathbb{R}$ times a disc D^4 and has a timelike conformal boundary $\mathcal{B} \cong \mathbb{R} \times S^3$ at $\theta = \pi/2$. As shown in Fig. 1.3(b) the past light cone of an observer sitting at $\theta = 0$ intersects $\mathcal{B}$ at a S^3. The spatial area of the light cone is $\sin^3\theta\,\Omega_3$ and decreases away from this S^3, by definition it is a light-sheet. So the information content across the light cone is bounded by the area of the S^3. Then translation along τ shows all the interior data is encoded on the conformal boundary $N_{\mathrm{AdS}} \leq A(\mathcal{B})/4$.

Most spacetimes do not possess these nice features of AdS. For instance, the holographic screen of a closed FRW universe is its apparent horizon lying in the interior. So the general notion that a bulk theory with gravity is dual to a boundary field theory without gravity may not be true. In the case of AdS, most checking of the correspondence was carried out in the regime of supergravity (the *weak form* in Table 1.1). The major goal there is to study nonperturbative dynamics of gauge theory using supergravity calculation. More realistic field models with no conformal invariance and less supersymmetries can be constructed by certain modification of the bulk geometry such as replacing the S^5 with some other Einstein manifold [22] or turning on additional flux other than F_5 [23]. On the flip side of the coin, much less work has been done to understand the bulk physics via boundary theory. Actually this is more in the spirit of the holographic principle. If our world is really a “hologram” as ’t Hooft and Susskind conjectured, then quantum gravity should have a dimensionally reduced description. Recently, some progress has been made in this direction, where massive string states on the pp-wave background (Penrose limit of the AdS space) can be constructed by the boundary field operators [24]. However, we find it is hard to understand conceptually the AdS/CFT correspondence in its *strong form*. This correspondence is basically a duality between closed and open string theories. But there exists an asymmetry in the sense that on the one hand we have a full type IIB closed string theory, on the other we only have a low energy approximation of the open string. We want to ask what happened to the higher open string modes, where are they? It is generally believed that open string theory is more fundamental than closed one, if massive closed string states can be made out of massless open string modes, can this construction be generalized to massive open string states? We regard this as an important question, but can not offer any clues.

As already mentioned, the large N limit of gauge theory is one of the major ideas behind the AdS/CFT correspondence, another insight which directly led to its formulation comes from modelling black holes by using D-branes in string theory. In Chapter 2, we present an original calculation of the thermodynamics of $\mathcal{N} = 4$ SYM theory [25] which describes the low energy excitations on a stack of D3-branes and compare it to the result obtained via gravity approach. This calculation clearly shows the strong/weak regime of this duality.

Chapter 2

Thermodynamics of $\mathcal{N} = 4$ Supersymmetric Yang-Mills Theory

2.1 Black Holes and D-Branes

Ever since the black hole entropy formula Eq. (1.5) was proposed, it has become a central puzzle in gravity physics—what is the *statistical origin* of this entropy? The best answer we currently have is to count the *internal microscopic states* of a black hole in string theory. In spite of being very successful for a large class of black holes, the string theoretical model is still a far cry from the four dimensional Schwarzschild black hole. The reason is that in string theory the arguments used to explain the entropy depend heavily on supersymmetry and only apply to the extremal or near-extremal case. This is a vast subject [27], we will only review the necessary background for our computation.

It was suggested more than a decade ago [28] that a Schwarzschild black hole can be viewed as a highly excited fundamental string. The density of the state $|n\rangle$ is $W \sim \exp(M_{\mathrm{s}}\alpha'^{\,1/2}) \sim \exp(\sqrt{n})$, so the corresponding entropy is $S = \ln W \sim \sqrt{n}$. If we make the string mass $M_{\mathrm{s}}^2 \sim n/\alpha'$ equal the black hole mass $M = r_{\mathrm{bh}}/2G$ and note that Newton's constant $G \sim g_{\mathrm{s}}^2\alpha'$ and $r_{\mathrm{bh}}^2 \sim \alpha'$, then the string coupling $g_s \sim n^{-1/4}$. This leads to the black hole entropy $S_{\rm bh} \sim r_{\rm bh}^2/G \sim \sqrt{n}$. So we see this identification provides a qualitative matching between the black hole entropy and the degeneracy of the string state. Since generally $n \gg 1$, this reasoning only works for weak coupling.

The first truly success came when Strominger and Vafa [29] constructed a class of five dimensional extremal black holes which is charged under the 2-form R-R field strength F_2 and the 2-form axion field strength $\tilde{H}_2$ arising from the NS-NS field strength H_3. When both charges Q_F and Q_H are non-vanishing, these black holes preserve 4 supersymmetries and have non-zero horizon area. Eq. (1.5) then gives the entropy $S_{\rm bh} = 2\pi\sqrt{Q_H Q_F^2/2}$. This result can be reproduced by considering a D1-D5 system or intersecting D3-branes which carry exactly the same set of charges as the black hole. Counting the state degeneracy, one obtains $S_{\rm stat} = 2\pi\sqrt{Q_H(Q_F^2/2+1)}$. So in the large charge limit, these two calculations agree with each other.

Even more interesting configurations are parallel Dp-branes, which are related to the black p-brane solutions in supergravity. For definiteness, we start with type II supergravity in ten dimensions. A black p-brane is a black hole charged under the $(p+2)$-form R-R field strength $F_{p+2} = dC_{p+1}$. In the string frame, the relevant part of the supergravity action is

$$I = \frac{1}{(2\pi)^7 l_s^8} \int d^{10}x \sqrt{-g} \left\{ e^{-2\phi} \left[R + 4(\nabla\phi)^2 \right] - \frac{2}{(8-p)!} F_{p+2}^2 \right\}. \qquad (2.1)$$

In type IIA (IIB) theory, p is even (odd). The string frame is related to the Einstein frame by $g_{\mu\nu}^{\rm E} = g_{\mu\nu}\sqrt{g_s e^{-\phi}}$, and this fixes the coefficient of the

Einstein-Hilbert action

$$(2\pi)^7 l_{\rm s}^8 g_{\rm s}^2 = 2\kappa^2 = 16\pi G = 16\pi \ell_{\rm p}^8. \tag{2.2}$$

We demand the Euclidean symmetry $ISO(p)$ along the p-brane and the spherical symmetry in the $(9-p)$ transverse directions. The R-R charge N is given by the Gauss' Law

$$\int_{S^{8-p}} *F_{p+2} = N. \tag{2.3}$$

In the string frame, the resulting metric and the dilaton field are [30]

$$ds^2 = -\frac{f_+(\rho)}{\sqrt{f_-(\rho)}}dt^2 + \sqrt{f_-(\rho)}d\vec{x}^{\,2} + \frac{f_-(\rho)^{-\frac{1}{2}-\frac{5-p}{7-p}}}{f_+(\rho)}d\rho^2 + \rho^2 f_-(\rho)^{\frac{1}{2}-\frac{5-p}{7-p}}d\Omega_{8-p}^2, \tag{2.4}$$

$$e^\phi = g_{\rm s} f_-(\rho)^{\frac{p-3}{4}}, \tag{2.5}$$

where $d\vec{x}^{\,2} = \sum_{i=1}^p (dx^i)^2$ and $f_\pm(\rho) = 1-(r_\pm/\rho)^{7-p}$. The two parameters $r_\pm$ are determined by the mass (density) M and the R-R charge N. There is a horizon at $\rho = r_+$, and a curvature singularity at $\rho = r_-$. To avoid the naked singularity, we require $r_+ \geq r_-$. This inequality leads to the so-called Bogomolnyi-Prasad-Sommerfield (BPS) relation between the mass and the charge

$$M \geq \frac{N}{(2\pi)^p g_{\rm s} l_{\rm s}^{p+1}}. \tag{2.6}$$

This charge N can be identified with the central charge of $\mathcal{N}=2$ supersymmetry of the type II supergravity. The BPS state which saturates the mass bound only preserves one half of the supersymmetry, and the corresponding p-brane is called *extremal*. For $p \neq 3$, the extremal solution has a "null" singularity at $r_+ = r_-$ where the supergravity description breaks down. It has been strongly believed that in the full string theory, the extremal p-brane is elevated to a new type of nonperturbative object: D-brane.

A Dp-brane is a hypersurface with $(p+1)$-dimensional worldvolume where open strings can end. Its existence in the nonperturbative string theory is required by duality and it provides the source for the R-R fields [31]. Open strings stuck on a Dp-brane satisfy the Dirichlet boundary condition in the $(9-p)$ transverse directions and the usual Neumann boundary condition along the worldvolume. The left and right movers on the open strings are related by the boundary condition, so the Dp-brane breaks at least one half of the 32 spacetime supercharges of the type II string. To be a BPS state, p has to be even (odd) in type IIA (IIB) theory. This is exactly the same as the extremal p-brane. D-branes are very heavy in the weak string coupling regime (see Eq. (2.6)), so they are not seen in the free string spectrum. Another way to get a large mass is to put N D-branes on top of each other (this accidently shows that small $g_{\rm s}$ is equivalent to large N), then this stack of branes carry N units of the R-R charge. This massive configuration will certainly curve the surrounding spacetime, which can be described by the metric Eq. (2.4) in the supergravity approximation.[1] It is clear that the D-branes can not be rigid because they will vibrate in response to the bulk gravitational wave (close string modes). This vibration can be described by the massless excitations of the open strings which wander on the branes. Since the open strings carry the Chan-Paton factors on their ends, for N coinciding Dp-branes we find the

[1]High order corrections (in α') to the metric have recently been studied in [32].

low energy effective theory to be a $(p+1)$-dimensional $U(N)$ gauge theory with 16 supercharges. Therefore, the stack of D-branes has dual descriptions as a gravitational soliton on the one hand and a SYM theory on the other. This suggests that we may explain the black hole entropy by studying the corresponding SYM theory.

To facilitate further discussion, we rewrite the black p-brane solution Eq. (2.4) and Eq. (2.5) as [21]

$$ds^2 = \frac{1}{\sqrt{H(r)}}\left[-f(r)dt^2 + d\vec{x}^{\,2}\right] + \sqrt{H(r)}\left[f^{-1}(r)dr^2 + r^2 d\Omega_{8-p}^2\right], \quad (2.7)$$

$$e^{\phi} = g_{\mathrm{s}} H(r)^{\frac{3-p}{4}}, \quad (2.8)$$

where

$$H(r) = 1 + \left(\frac{L}{r}\right)^{7-p} \quad \text{and} \quad f(r) = 1 - \left(\frac{r_0}{r}\right)^{7-p}. \quad (2.9)$$

The two parameters L and r_0 are related to $r_{\pm}$. The horizon is now located at $r = r_0$ and the p-brane becomes extremal when $r_0 = 0$. For the extremal brane, $f(r) = 1$, so the Euclidean symmetry $ISO(p)$ is enhanced to the Poincaré symmetry $ISO(1,p)$ on the worldvolume. From the metric, we can read off the horizon area

$$A = H(r_0)^{-\frac{p}{4}} V_p \left[H(r_0)^{\frac{1}{4}} r_0\right]^{8-p} \Omega_{8-p} \simeq \left(\frac{L}{r_0}\right)^{\frac{(7-p)(4-p)}{2}} r_0^{8-p} V_p \Omega_{8-p}, \quad (2.10)$$

where V_p is the spatial volume of the p-brane. The second equality holds for the near-extremal brane ($r_0 \ll L$). It is easy to check for $p = 2, \cdots, 7$, r_0 has a positive power. So the horizon area vanishes in the extremal limit and the black hole entropy is zero according to the area formula Eq. (1.5). This can be understood by noting that the corresponding D-brane configuration is in its ground state. When the p-brane is excited slightly above the extremality, the stack of D-branes also starts to have open string oscillations on it. When heated up to the same temperature, the SYM gas is expected to account for the black hole entropy.

One special solution which deserves our attention is when $p = 3$. As can be seen, the dilaton is a constant in this case. So we can eliminate the string loop correction by setting g_{s} small everywhere. The extremal 3-brane has a metric

$$ds^2 = \left(1 + \frac{L^4}{r^4}\right)^{-1/2} \left(-dt^2 + d\vec{x}^2\right) + \left(1 + \frac{L^4}{r^4}\right)^{1/2} \left(dr^2 + r^2 d\Omega_5^2\right), \quad (2.11)$$

which is non-singular near the horizon $r = 0$. In fact, the near-horizon geometry is

$$ds^2 = \frac{r^2}{L^2} \left(-dt^2 + d\vec{x}^2\right) + L^2 \frac{dr^2}{r^2} + L^2 d\Omega_5^2. \quad (2.12)$$

This metric describes $AdS_5 \times S^5$ (see Fig. 2.1(a)), both factors are maximally symmetric. The AdS part actually only covers one half of AdS_5, the so-called *Poincaré patch* (see Fig. 2.1(b)). It can be rewritten in two other frequently used forms:

$$ds^2_{\text{Poincaré}} = \frac{L^2}{z^2} \left(-dt^2 + d\vec{x}^2 + dz^2\right) \qquad r = L^2/z, \quad (2.13)$$

$$ds^2_{\text{Poincaré}} = e^{-2u/L} \left(-dt^2 + d\vec{x}^2\right) + du^2 \qquad r = Le^{-u/L}. \quad (2.14)$$

The scale factor L for the extremal p-brane is given by [21]

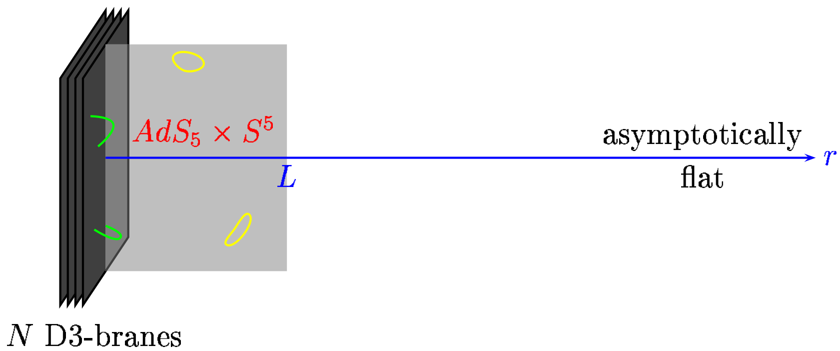

(a) D3-brane geometry

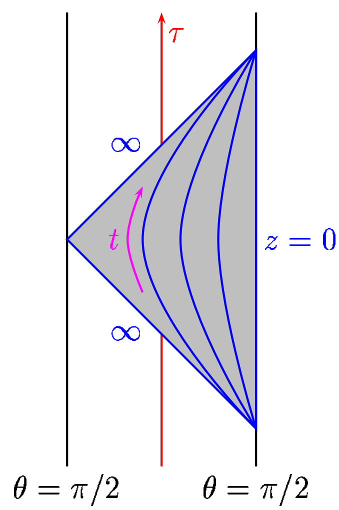

(b) Poincaré patch

Figure 2.1: The surrounding spacetime structure of N coinciding D3-branes: (a) shows the full geometry, where open strings move on the D3-branes and closed strings propagate in the bulk; (b) is the Penrose diagram of the near-horizon geometry.

$$L^{7-p} = 2^{5-p}\pi^{\frac{5-p}{2}}\Gamma\left(\frac{7-p}{2}\right) g_{\rm s} N l_{\rm s}^{7-p}. \tag{2.15}$$

So we have $L^4 = 4\pi g_{\rm s} N\alpha'^2$ for the 3-brane. As already mentioned in Chapter 1, $g_{\rm s}$ is related to the Yang-Mills coupling via $4\pi g_{\rm s} = g_{\rm YM}^2$. Then in terms of the 't Hooft coupling $\lambda = g_{\rm YM}^2 N$, we get

$$L^4 = \lambda\alpha'^2. \tag{2.16}$$

The supergravity calculation is reliable when the spacetime curvature R is small. Since $R \sim 1/L^2$, we require $L^2 \gg \alpha'$ in order to suppress the string α' correction. So the supergravity description of the stack of D3-branes is relevant to the SYM theory in the *strong* 't Hooft coupling regime $\lambda \gg 1$.

We now compute the entropy of the near-extremal black hole whose horizon area is non-vanishing. The near-horizon geometry can be obtained from Eq. (2.7) by plugging in $H(r) \simeq (L/r)^4$:

$$ds^2 = \frac{r^2}{L^2}\left[-\left(1-\frac{r_0^4}{r^4}\right)dt^2 + d\vec{x}^2\right] + \frac{L^2}{r^2}\left(1-\frac{r_0^4}{r^4}\right)^{-1} dr^2 + L^2 d\Omega_5^2. \tag{2.17}$$

This can be identified with a S^5 times a certain limit of the five-dimensional Schwarzschild-AdS black hole [33]. Eq. (2.10) gives the horizon area $A = L^2 r_0^3 V_3 \Omega_5$. The Hawking temperature can be calculated by a Euclidean continuation of the time [34] and turns out to be $\beta = \pi L^2/r_0$. So the black hole entropy is [35]

$$S_{\rm bh} = \frac{A}{4G} = \frac{L^2\left(\pi L^2 T\right)^3 V_3 \pi^3}{32\pi^6\alpha'^4 g_{\rm s}^2} = \frac{\pi^2}{2} N^2 T^3 V_3, \tag{2.18}$$

where we have used Eq. (2.2) and $\Omega_5 = \pi^3$. How is this compared to the SYM gas heated up to the same temperature? The gauge theory on the D3-branes is the $\mathcal{N}=4$ $U(N)$ SYM theory. This can be understood by using dimensional reduction. We start with type I open string in ten dimensions. Its low energy effective theory is a SYM theory with 16 supercharges. All the boundary conditions on the open string ends are Neumann, so the spacetime itself can be regarded as a D9-brane. Now if we make a T-duality transformation along x^9-direction, the D9-brane will turn into a D8-brane since T-duality interchange the Neumann and Dirichlet boundary conditions. This D8-brane sits at some fixed x^9 position and the open strings can only move in the remaining nine-dimensional spacetime. The A_9 component of the original gauge field becomes a Higgs field which denotes the transverse location of the D8-brane. Keeping T-dualizing x^8 through x^4 directions, we finally get the four-dimensional maximally supersymmetric Yang-Mills theory. The $U(N)$ gauge symmetry comes in when we put N copies of D3-branes on top of each other. This SYM theory consists of two real gauge degrees of freedom, six scalars corresponding to the six transverse coordinates and eight fermions which are the goldstinoes associated with the broken supersymmetry. To the lowest order ($g_{\rm YM}=0$), the statistical mechanics is that of a free SYM gas. Its partition function is given by

$$Z_0 = Z_{\rm B}^{N_{\rm B}} Z_{\rm F}^{N_{\rm F}}, \tag{2.19}$$

where

$$\ln Z_{\rm B} = V_3 \int \frac{d^3p}{(2\pi)^3} \ln\left(1-e^{-\beta p}\right)^{-1} = \frac{\pi^2}{90} T^3 V_3, \tag{2.20}$$

$$\ln Z_{\rm F} = V_3 \int \frac{d^3p}{(2\pi)^3} \ln\left(1+e^{-\beta p}\right) = \frac{7}{8}\frac{\pi^2}{90} T^3 V_3. \tag{2.21}$$

After plugging in the bosonic and fermionic degrees of freedom $N_{\rm B} = N_{\rm F} = 8N^2$, we get the free energy

$$F_0 = -T \ln Z_0 = -\frac{\pi^2}{90}\left(N_{\rm B} + \frac{7}{8}N_{\rm F}\right) T^4 V_3 = -\frac{\pi^2}{6} N^2 T^4 V_3. \qquad (2.22)$$

So the free SYM gas has an entropy

$$S_0 = -\frac{\partial F_0}{\partial T} = \frac{2\pi^2}{3} N^2 T^3 V_3. \qquad (2.23)$$

Comparing to the black hole entropy, we see $S_{\rm bh} = 3S_0/4$. As has been pointed out, the supergravity calculation is only valid in the strong 't Hooft coupling regime; while perturbative SYM calculation necessarily assumes weak coupling. So these two results are at two different ends of the parameter space of λ. This illustrates the strong/weak duality of the AdS/CFT correspondence.

It is natural to pursue the calculation to the next order at both ends. In particular, we want to know whether the free energy as a function of λ can be continued smoothly from one end to the other. On the gravity side, the correction due to the $\alpha'^3 R^4$ term has been computed in [36]. In the Einstein frame, the tree level type II effective action Eq. (2.1) receives the first correction at α'^3 level [37]

$$\Delta I^{\rm E} = \frac{1}{16\pi G}\int d^{10}x\sqrt{-g}\left[\frac{1}{8}\zeta(3)\alpha'^3 e^{-\frac{3}{2}\phi} W + \cdots\right], \qquad (2.24)$$

where W is a function of the Weyl tensor raised to the fourth power. The action for the five-dimensional black hole is obtained by compactifying on S^5. It is not hard to see how the correction to the free energy scales with λ. In

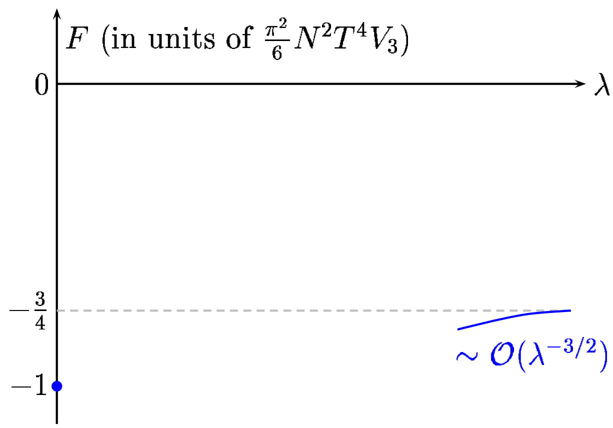

Figure 2.2: The free energy of $\mathcal{N}=4$ $U(N)$ SYM theory as a function of the 't Hooft coupling λ.

the Euclidean gravity approach, the free energy is related to the Euclidean gravitational action by

$$F = -T\ln Z = -T\ln e^{-\mathcal{I}} = T\mathcal{I}. \tag{2.25}$$

Since $\Delta\mathcal{I} \propto \alpha'^3 \propto \lambda^{-3/2}$, we find $\Delta F \propto \lambda^{-3/2}T^4V_3$. More precisely, the free energy of $\mathcal{N}=4$ $U(N)$ SYM theory can be cast in the following form:

$$F = -\frac{\pi^2}{6}f(\lambda)N^2T^4V_3, \tag{2.26}$$

where

$$f(\lambda) = \begin{cases} 1 & \text{when} \quad \lambda = 0, \\ \frac{3}{4} + \frac{45}{32}\zeta(3)(2\lambda)^{-3/2} + \cdots & \text{when} \quad \lambda \gg 1. \end{cases} \tag{2.27}$$

From this expression, one might be tempted to conjecture that $f(\lambda)$ is a monotonically decreasing function interpolating between the weak and the strong 't Hooft coupling (see Fig. 2.2). To check whether this is true, we need to go beyond the free gas approximation and compute the higher order correction in the perturbation theory. In the next section, we will calculate the free energy at two-loop level. The result which we obtain preceded [26] by about one month.

2.2 Two-Loop Calculation of the Free Energy

To carry out the diagrammatic calculation, we need to first develop some basic machinery in finite-temperature field theory (see, for instance, [38]). A thermodynamical system can be generally described by an Hamiltonian $H[\phi, \pi]$, where $\phi(x)$ is the field[2] and $\pi(x)$ is its conjugate momentum. The partition function of the system is defined as the trace of its density matrix

$$Z = \mathrm{Tr}\, e^{-\beta H} = \sum_n \langle \phi_n | e^{-\beta H} | \phi_n \rangle, \tag{2.28}$$

where n runs over the entire Hilbert space. We can rewrite Z in the path integral formulation. Recall the transition amplitude from state $|\phi_a\rangle$ at time t_a to state $|\phi_b\rangle$ at time t_b:

$$\langle \phi_b | e^{-iH(t_b - t_a)} | \phi_a \rangle = \int \mathcal{D}\pi \mathcal{D}\phi \exp\left\{ i \int_{t_a}^{t_b} dt \int d^3x \left[\pi \partial_t \phi - \mathcal{H}(\phi, \pi) \right] \right\}. \tag{2.29}$$

After Wick-rotation $it \to \tau$, $\partial_t \phi \to i\partial_\tau \phi$ and substituting into Eq. (2.28), we get

$$Z = \int_{\text{periodic}\,\phi} \mathcal{D}\pi \mathcal{D}\phi \exp\left\{ \int_0^\beta d\tau \int d^3x \left[i\pi \partial_\tau \phi - \mathcal{H}(\phi, \pi) \right] \right\}, \tag{2.30}$$

[2]We have suppressed all the spacetime indexes here, so ϕ can be a scalar, vector or spinor field.

where $\beta = i(t_b - t_a)$ is the period of the Euclidean time since the initial and final states are identical in the trace. Usually the Hamiltonian density $\mathcal{H}(\phi, \pi)$ is quadratic in π, so we can perform the Gaussian integration over π explicitly. This turns the Hamiltonian path integral into the Lagrangian form

$$Z = N(\beta) \int_{\text{periodic}} \mathcal{D}\phi \exp \underbrace{\left\{ \int_0^\beta d\tau \int d^3x \mathcal{L}(\phi, i\partial_\tau \phi) \right\}}_{I_0 + I_{\text{int}}} \tag{2.31}$$

where we have split the action into the free and the interaction parts ($I = -\mathcal{I}$ for the Euclidean action). The π integration generates an awkward temperature dependent infinite constant $N(\beta)$. In zero-temperature field theory, this is not a problem since $N(\beta)$ drops out in the calculation of the correlation function $\langle \mathcal{O}_1 \cdots \mathcal{O}_n \rangle / Z$. As shown by Bernard [39], the temperature part in $N(\beta)$ is actually cancelled by some factors in the functional determinant (see below) after a careful discretization of the path integral, so we are in good shape again. Then it is straightforward to compute the free energy using perturbative expansion

$$\begin{aligned}
F &= -T \ln Z = -T \ln \left[N(\beta) \int \mathcal{D}\phi e^{I_0} \frac{\int \mathcal{D}\phi e^{I_0} \left(1 + I_{\text{int}} + \frac{1}{2} I_{\text{int}}^2 + \cdots \right)}{\int \mathcal{D}\phi e^{I_0}} \right] \\
&= -T \left\{ \ln \left(N(\beta) \int \mathcal{D}\phi e^{I_0} \right) + \ln \left[\frac{\int \mathcal{D}\phi e^{I_0} \left(1 + I_{\text{int}} + \frac{1}{2} I_{\text{int}}^2 + \cdots \right)}{\int \mathcal{D}\phi e^{I_0}} \right] \right\} \\
&= -T \ln Z_0 - T \ln \left(1 + \frac{\int \mathcal{D}\phi e^{I_0} I_{\text{int}}}{\int \mathcal{D}\phi e^{I_0}} + \frac{1}{2} \frac{\int \mathcal{D}\phi e^{I_0} I_{\text{int}}^2}{\int \mathcal{D}\phi e^{I_0}} + \cdots \right) \\
&= -T \ln Z_0 - T \left(\frac{\int \mathcal{D}\phi e^{I_0} I_{\text{int}}}{\int \mathcal{D}\phi e^{I_0}} + \frac{1}{2} \frac{\int \mathcal{D}\phi e^{I_0} I_{\text{int}}^2}{\int \mathcal{D}\phi e^{I_0}} + \cdots \right).
\end{aligned} \tag{2.32}$$

The first term (one-loop functional determinant) $F_0 = -T \ln Z_0$ gives the free energy of a free gas, Eq. (2.22); while the terms in the bracket are higher loop corrections, among which the first two correspond to the two-loop level.

Because of the periodicity in the imaginary time, energy is quantized

$$\omega_n = \frac{2\pi n}{\beta} \qquad \begin{cases} n \in \mathbb{Z} & \text{boson,} \\ n \in \mathbb{Z} + \frac{1}{2} & \text{fermion.} \end{cases} \tag{2.33}$$

So the integration over p_0 is replaced with the summation over ω_n. Fermions satisfy the anti-periodic boundary condition since they pick up a minus sign after 2π rotation along τ. Note that the ghosts also have integer frequencies because they are scalars under Lorentz transformation despite being anti-commutative. We can summarize the basic rules of Feynman diagram calculation in finite-temperature field theory:

zero-temperature	finite-temperature
p_0	$i\omega_n$
$\int \frac{d^4p}{(2\pi)^4}$	$\frac{1}{\beta}\sum_n \int \frac{d^3p}{(2\pi)^3}$
usual propagator $\times i$	thermal propagator
usual vertex $\times(-i)$	thermal vertex

Table 2.1: Comparisons between the ordinary field theory and thermal field theory.

As discussed in Section 2.1, the Lagrangian of $\mathcal{N}=4$ $D=4$ $U(N)$ SYM theory can be obtained from the dimensional reduction of $\mathcal{N}=1$ $D=10$ $U(N)$ SYM theory

$$I_{(10)} = \int d^{10}x \left(-\frac{1}{4} F^a_{\rho\sigma} F^{\rho\sigma a} + \frac{1}{2} i \overline{\eta}^a \Gamma \cdot D \eta^a \right). \tag{2.34}$$

It is easy to write down the bosonic part first. We rename A_i $(i = 4, \cdots, 9)$

as ϕ_i in the four-dimensional theory:

$$\mathcal{L}_{\rm B} = -\frac{1}{4}F^a_{\mu\nu}F^{\mu\nu a} + \frac{1}{2}D_\mu\phi^{ia}D^\mu\phi^{ia} - \frac{1}{4}g^2_{\rm YM}(f^{eab}\phi^{ia}\phi^{jb})(f^{ecd}\phi^{ic}\phi^{jd}), \quad (2.35)$$

where

$$\begin{cases} F^a_{\mu\nu} = \partial_\mu A^a_\nu - \partial_\nu A^a_\mu + g_{\rm YM}f^{abc}A^b_\mu A^c_\nu & (\mu,\, \nu = 0, \cdots, 3), \\ F^a_{\mu i} = \partial_\mu \phi^a_i + g_{\rm YM}f^{abc}A^b_\mu \phi^c_i \equiv D_\mu\phi^a_i & (i,\, j = 4, \cdots, 9), \\ F^a_{ij} = g_{\rm YM}f^{abc}\phi^b_i\phi^c_j. \end{cases} \quad (2.36)$$

As usual, to fix the gauge, we introduce the ghost fields c and $\overline{c}$

$$\mathcal{L}_{\rm gh} = \overline{c}^a(-\partial^2\delta^{ac} - g_{\rm YM}\partial^\mu f^{abc}A^b_\mu)c^c. \quad (2.37)$$

In Feynman gauge ($\xi = 1$), the bare thermal propagators and vertices are listed in Fig. 2.3.

The fermionic part of the Lagrangian can be written down by finding a suitable representation of the (32×32) Γ matrices in terms of the (4×4) γ matrices and also the $D = 10$ Majorana-Weyl spinor η in terms of the $D = 4$ Dirac spinor χ. Following [40], we choose

$$\begin{array}{ll} \Gamma^\mu = \gamma^\mu \otimes I_8 & (\mu = 0, \cdots, 3), \\ \Gamma^{ij} = \gamma^5 \otimes \begin{pmatrix} 0 & \rho^{ij} \\ \rho_{ij} & 0 \end{pmatrix} & (i,\, j = 1, \cdots, 4), \\ \Gamma_{11} = \Gamma_0\Gamma_1\cdots\Gamma_9 = \gamma^5 \otimes \begin{pmatrix} I_4 & 0 \\ 0 & I_4 \end{pmatrix}, & \end{array} \quad (2.38)$$

where

$$\begin{array}{l} (\rho^{ij})_{kl} = \delta_{ik}\delta_{jl} - \delta_{jk}\delta_{il}, \\ (\rho_{ij})_{kl} = \frac{1}{2}\epsilon_{ijmn}(\rho^{mn})_{kl} = \epsilon_{ijkl}. \end{array} \quad (2.39)$$

The Majorana-Weyl spinor η satisfies $\Gamma_{11}\eta = \eta$ and $\eta = C_{10}\overline{\eta}^{\rm T}$ by definition. And the ten-dimensional charge conjugation operator is

$$C_{10} = C_4 \otimes \begin{pmatrix} 0 & I_4 \\ I_4 & 0 \end{pmatrix}. \quad (2.40)$$

gluon 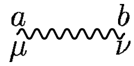

$$-\frac{g^{\mu\nu}\delta^{ab}}{\omega_n^2+\vec{p}^{\,2}}$$

scalar 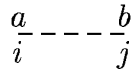

$$\frac{\delta^{ij}\delta^{ab}}{\omega_n^2+\vec{p}^{\,2}}$$

ghost 

$$\frac{\delta^{ab}}{\omega_n^2+\vec{p}^{\,2}}$$

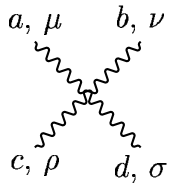

$$\begin{aligned}-g_{\rm YM}^2[&f^{abe}f^{cde}(g^{\mu\rho}g^{\nu\sigma}-g^{\mu\sigma}g^{\nu\rho})\\ &+f^{ace}f^{bde}(g^{\mu\nu}g^{\rho\sigma}-g^{\mu\sigma}g^{\nu\rho})\\ &+f^{ade}f^{bce}(g^{\mu\nu}g^{\rho\sigma}-g^{\mu\rho}g^{\nu\sigma})]\end{aligned}$$

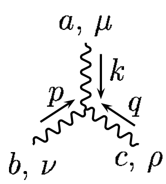

$$\begin{aligned}-ig_{\rm YM}f^{abc}[g^{\mu\nu}(k-p)^\rho+g^{\nu\rho}(p-q)^\mu&\\ +g^{\rho\mu}(q-k)^\nu]&\end{aligned}$$

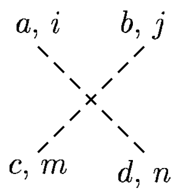

$$\begin{aligned}-g_{\rm YM}^2[&f^{abe}f^{cde}(\delta^{im}\delta^{jn}-\delta^{in}\delta^{jm})\\ &+f^{ace}f^{bde}(\delta^{ij}\delta^{mn}-\delta^{in}\delta^{jm})\\ &+f^{ade}f^{bce}(\delta^{ij}\delta^{mn}-\delta^{im}\delta^{jn})]\end{aligned}$$

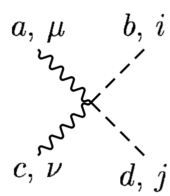

$$g_{\rm YM}^2(f^{abe}f^{cde}-f^{ade}f^{bce})g^{\mu\nu}\delta^{ij}$$

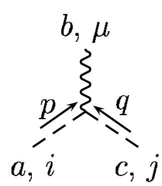

$$ig_{\rm YM}f^{abc}\delta^{ij}(p-q)^\mu$$

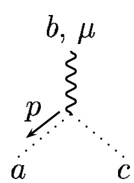

$$ig_{\rm YM}f^{abc}p^\mu$$

Figure 2.3: Bosonic Feynman rules.

Then it is not hard to check the following spinor η does satisfy the Majorana-Weyl condition

$$\eta = \begin{pmatrix} L\chi^i \\ R\widetilde{\chi}_i \end{pmatrix} \qquad \widetilde{\chi}_i = C_4(\overline{\chi}^i)^{\mathrm{T}} \qquad (i = 1, \cdots, 4), \tag{2.41}$$

where L and R are the projection operators in four dimensions

$$L = \frac{1}{2}(1+\gamma_5) = \begin{pmatrix} I_2 & 0 \\ 0 & 0 \end{pmatrix} \qquad R = \frac{1}{2}(1-\gamma_5) = \begin{pmatrix} 0 & 0 \\ 0 & I_2 \end{pmatrix}. \tag{2.42}$$

Now rewrite the six scalars as

$$\phi^a_{i4} = \frac{1}{\sqrt{2}}(A^a_{i+3} + iA^a_{i+6}) \quad \phi^{jka} = \frac{1}{2}\epsilon^{jklm}\phi^a_{lm} = (\phi^a_{jk})^* \quad (i = 1,2,3), \tag{2.43}$$

so they transform as a **6** of the $SU(4)$ R-symmetry. Upon plugging in Eq. (2.34), the resulting fermionic Lagrangian is

$$\mathcal{L}_{\mathrm{F}} = i\overline{\chi}^a\gamma\cdot DL\chi^a - \frac{1}{2}ig_{\mathrm{YM}}f^{abc}(\overline{\widetilde{\chi}}^{ia}L\chi^{jb}\phi^c_{ij} - \overline{\chi}^a_i R\widetilde{\chi}^b_j\phi^{ijc}). \tag{2.44}$$

We can go one step further by writing the Dirac spinor χ in terms of the two-dimensional Weyl spinor ψ, $\chi^i = (\psi^i\ \zeta^i)^{\mathrm{T}}$. Then the above equation becomes

$$\mathcal{L}_{\mathrm{F}} = i\psi^{ia\dagger}\overline{\sigma}\cdot D\psi^{ia} - \frac{1}{2}g_{\mathrm{YM}}f^{abc}(\psi^{ia\dagger}\sigma^2\psi^{jb}\phi^c_{ij} + \psi^{a\dagger}_i\sigma^2\psi^b_j\phi^{ijc}). \tag{2.45}$$

This is the form we use to perform the fermionic calculation. Again, the bare thermal propagator and vertices can be read off of the Lagrangian (Fig. 2.4). Note the Pauli matrices $\sigma^\mu = (1, \sigma^i)$ and $\overline{\sigma}^\mu = (1, -\sigma^i)$ satisfy

$$\{\overline{\sigma}^\mu, \sigma^\nu\} = 2\eta^{\mu\nu} + 2(\delta^\mu_0\delta^\nu_i - \delta^\nu_0\delta^\mu_i)\sigma^i, \tag{2.46}$$

which will be used when computing the traces. Using these Feynman rules, we

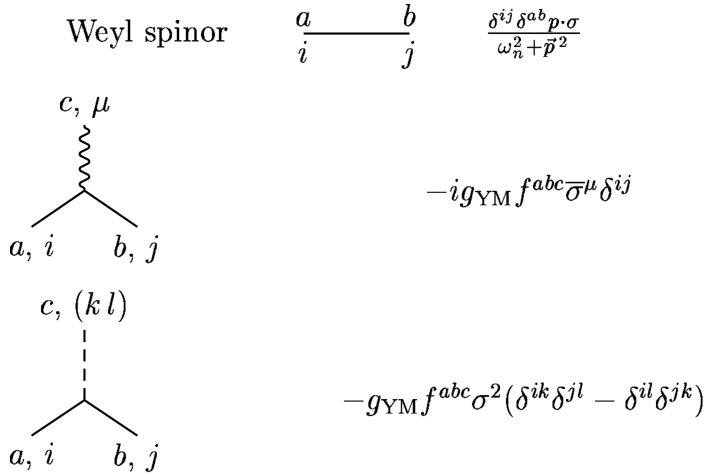

Figure 2.4: Fermionic Feynman rules.

can write down six bosonic and two fermionic diagrams at the two-loop level. Therefore, the corresponding two-loop contribution to the free energy is

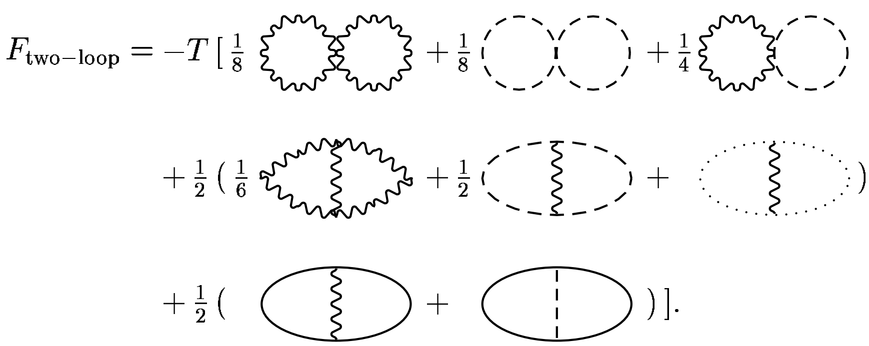

(2.47)

The first three diagrams come from the first bracketed term in Eq. (2.32); the rest five ones come from the second term, note the overall coefficient 1/2. We also include various symmetry factors for each diagram.

Before launching into the detailed calculation, we make one more remark on the cancellation of the many infinities which appear in loop integration. From the supersymmetry algebra[3]

$$\{Q_\alpha, \overline{Q}_{\dot\beta}\} = 2\sigma^\mu_{\alpha\dot\beta} P_\mu, \tag{2.48}$$

it can be seen that the Hamiltonian is non-negative

$$4\langle\psi|P^0|\psi\rangle = \langle\psi|Q_\alpha(Q_\alpha)^* + (Q_\alpha)^* Q_\alpha|\psi\rangle \geq 0. \tag{2.49}$$

So if the vacuum is invariant under supersymmetry transformation ($Q_\alpha|0\rangle = 0$), the vacuum energy has to vanish. Since $F = E - TS$, all the infinities must cancel out in the limit $T \to 0$. This serves as a check of our calculation.

We claim all the calculations can be reduced to two basic summation-integrations:

$$\mathcal{B} = \int_{\mathrm{B}} \frac{d^4p}{(2\pi)^4} \frac{1}{p^2} \equiv \frac{1}{\beta} \sum_{n\in\mathbb{Z}} \int \frac{d^3p}{(2\pi)^3} \frac{1}{\omega_n^2 + \vec{p}^{\,2}}, \tag{2.50}$$

$$\mathcal{F} = \int_{\mathrm{F}} \frac{d^4p}{(2\pi)^4} \frac{1}{p^2} \equiv \frac{1}{\beta} \sum_{n\in\mathbb{Z}+\frac{1}{2}} \int \frac{d^3p}{(2\pi)^3} \frac{1}{\omega_n^2 + \vec{p}^{\,2}}. \tag{2.51}$$

The energy summation can be done via Sommerfeld-Watson transformation [41] (basically a contour integration, see Appendix A)

$$\sum_n \frac{1}{\omega_n^2 + \vec{p}^{\,2}} = \frac{\beta}{2p} \cdot \begin{cases} \coth\left(\frac{1}{2}\beta p\right) & n \in \mathbb{Z}, \\ \tanh\left(\frac{1}{2}\beta p\right) & n \in \mathbb{Z} + \frac{1}{2}. \end{cases} \tag{2.52}$$

Clearly both $\mathcal{B}$ and $\mathcal{F}$ are divergent. However, we argue that the physically meaningful quantity is the difference between the finite-temperature result and

[3] This is the $\mathcal{N} = 1$ version. The same argument goes through for $\mathcal{N} = 4$ since we are only considering the superconformal phase.

its zero-temperature counterpart because it can be shifted by any temperature independent constant. The "renormalized" $\mathcal{B}$ and $\mathcal{F}$ are indeed finite

$$\mathcal{B}_{\rm R} = \mathcal{B} - \mathcal{B}(\beta \to \infty) = \mathcal{B} - \frac{1}{\pi^2}\int_0^\infty dp\, p = \frac{T^2}{12}, \tag{2.53}$$

$$\mathcal{F}_{\rm R} = \mathcal{F} - \mathcal{F}(\beta \to \infty) = \mathcal{F} - \frac{1}{\pi^2}\int_0^\infty dp\, p = -\frac{T^2}{24}. \tag{2.54}$$

So we can divide $\mathcal{B}$ and $\mathcal{F}$ into a finite piece plus infinity

$$\mathcal{B} = \frac{T^2}{12} + \infty^2 \qquad \mathcal{F} = -\frac{T^2}{24} + \infty^2, \tag{2.55}$$

where the quadratic divergence denotes the p integration.

We now justify the basic claim Eqs. (2.50) and (2.51). A general bosonic two-loop diagram involves a summation-integration like

$$\int_{\rm B} \frac{d^4p}{(2\pi)^4} \int_{\rm B} \frac{d^4q}{(2\pi)^4} \frac{p^2 + q^2 + p\cdot q}{p^2q^2(p+q)^2}. \tag{2.56}$$

It is easy to compute the first two terms by a simple shift of the integration variable and they are $2\mathcal{B}^2$. The cross term containing $p \cdot q$ is much harder. We use a trick here by constructing an identity:

$$\int_{\rm B} \frac{d^4p}{(2\pi)^4} \int_{\rm B} \frac{d^4q}{(2\pi)^4} \frac{(p+q)^2}{p^2q^2(p+q)^2} \equiv \int_{\rm B} \frac{d^4p}{(2\pi)^4} \int_{\rm B} \frac{d^4q}{(2\pi)^4} \frac{p^2 + q^2 + 2p\cdot q}{p^2q^2(p+q)^2}.$$

The left hand side (LHS) of the identity is just $\mathcal{B}^2$ by definition; the right hand side (RHS) is $2\mathcal{B}^2$ again plus twice the cross term. So we have

$$\int_{\rm B} \frac{d^4p}{(2\pi)^4} \int_{\rm B} \frac{d^4q}{(2\pi)^4} \frac{p\cdot q}{p^2q^2(p+q)^2} = -\frac{1}{2}\mathcal{B}^2. \tag{2.57}$$

This result can be checked by a brute-force calculation of

$$\frac{1}{\beta^2}\sum_{n,m\in\mathbb{Z}}\int\frac{d^3p}{(2\pi)^3}\frac{d^3q}{(2\pi)^3}\frac{\vec{p}\cdot\vec{q}+\omega_n\omega_m}{(\omega_n^2+\vec{p}^{\,2})(\omega_m^2+\vec{q}^{\,2})[\omega_{n+m}^2+(\vec{p}+\vec{q})^2]}. \tag{2.58}$$

We first perform the two summations by using the same contour integration method as before (Appendix A)

$$\begin{aligned}
&\sum_{n,m\in\mathbb{Z}}\frac{1}{(n^2+p^2)(m^2+q^2)[(n+m)^2+k^2]}\\
&=\frac{2\pi^2}{(q^2-p^2-k^2)^2-4p^2k^2}\\
&\quad+\frac{\pi^2\coth p\pi\,\coth k\pi}{pk}\frac{q^2-p^2-k^2}{(q^2-p^2-k^2)^2-4p^2k^2}\\
&\quad+\frac{\pi^2\coth q\pi\,\coth k\pi}{qk}\frac{p^2-q^2-k^2}{(p^2-q^2-k^2)^2-4q^2k^2}\\
&\quad+\frac{\pi^2\coth p\pi\,\coth q\pi}{pq}\frac{k^2-p^2-q^2}{(k^2-p^2-q^2)^2-4p^2q^2},
\end{aligned} \tag{2.59}$$

$$\begin{aligned}
&\sum_{n,m\in\mathbb{Z}}\frac{n\,m}{(n^2+p^2)(m^2+q^2)[(n+m)^2+k^2]}\\
&=\frac{\pi^2(p^2+q^2-k^2)}{(q^2+k^2-p^2)^2-4q^2k^2}\\
&\quad+\frac{p\pi^2\coth p\pi\,\coth k\pi}{k}\frac{k^2+q^2-p^2}{(k^2+p^2-q^2)^2-4p^2k^2}\\
&\quad+\frac{q\pi^2\coth q\pi\,\coth k\pi}{k}\frac{k^2+p^2-q^2}{(k^2+q^2-p^2)^2-4q^2k^2}\\
&\quad-\frac{2p\pi\,q\pi\,\coth p\pi\,\coth q\pi}{(k^2-p^2-q^2)^2-4p^2q^2}.
\end{aligned} \tag{2.60}$$

The results are manifestly symmetric in p and q as they should be. Then substituting $\vec{k}=\vec{p}+\vec{q}$ and integrating over $\vec{p}$ and $\vec{q}$, we get $-\mathcal{B}^2/2$ (Appendix B).

We next turn to the fermionic two-loop diagrams. Just like the bosonic case, the hard part is to compute the cross term. The old trick works again with a new subtlety. We consider the identity:

$$\int_{\mathrm{F}} \frac{d^4p}{(2\pi)^4} \int_{\mathrm{F}} \frac{d^4q}{(2\pi)^4} \frac{(p-q)^2}{p^2q^2(p-q)^2} = \int_{\mathrm{F}} \frac{d^4p}{(2\pi)^4} \int_{\mathrm{F}} \frac{d^4q}{(2\pi)^4} \frac{p^2+q^2-2p\cdot q}{p^2q^2(p-q)^2}.$$

By definition the LHS is $\mathcal{F}^2$. The first two terms on the RHS are $2\mathcal{B}\mathcal{F}$ instead of $2\mathcal{F}^2$. The reason is that the momentum flow $(p-q)$ is carried by a boson (both p and q are carried by the fermions). Indeed from the two fermionic diagrams, we see it is either a gauge boson or a scalar. So the fermionic cross term is

$$\int_{\mathrm{F}} \frac{d^4p}{(2\pi)^4} \int_{\mathrm{F}} \frac{d^4q}{(2\pi)^4} \frac{p\cdot q}{p^2q^2(p-q)^2} = \mathcal{B}\mathcal{F} - \frac{1}{2}\mathcal{F}^2. \tag{2.61}$$

Parallel to the previous discussion, a direct check can be made for

$$\frac{1}{\beta^2} \sum_{n,m\in\mathbb{Z}+\frac{1}{2}} \int \frac{d^3p}{(2\pi)^3} \frac{d^3q}{(2\pi)^3} \frac{\vec{p}\cdot\vec{q}+\omega_n\omega_m}{(\omega_n^2+\vec{p}^2)(\omega_m^2+\vec{q}^2)[\omega_{n-m}^2+(\vec{p}-\vec{q})^2]}.$$

The two summations are

$$\begin{aligned}
&\sum_{n,m\in\mathbb{Z}+\frac{1}{2}} \frac{1}{(n^2+p^2)(m^2+q^2)[(n-m)^2+k^2]} \\
&= \frac{2\pi^2}{(q^2-p^2-k^2)^2-4p^2k^2} \\
&\quad + \frac{\pi^2 \tanh p\pi\, \coth k\pi}{pk} \frac{q^2-p^2-k^2}{(q^2-p^2-k^2)^2-4p^2k^2} \\
&\quad + \frac{\pi^2 \tanh q\pi\, \coth k\pi}{qk} \frac{p^2-q^2-k^2}{(p^2-q^2-k^2)^2-4q^2k^2} \\
&\quad + \frac{\pi^2 \tanh p\pi\, \tanh q\pi}{pq} \frac{k^2-p^2-q^2}{(k^2-p^2-q^2)^2-4p^2q^2},
\end{aligned} \tag{2.62}$$

$$
\begin{aligned}
&\sum_{n,m\in\mathbb{Z}+\frac{1}{2}} \frac{n\,m}{(n^2+p^2)(m^2+q^2)[(n-m)^2+k^2]} \\
&= -\frac{\pi^2(p^2+q^2-k^2)}{(q^2+k^2-p^2)^2-4q^2k^2} \\
&\quad -\frac{p\pi^2\tanh p\pi\ \coth k\pi}{k}\frac{k^2+q^2-p^2}{(k^2+p^2-q^2)^2-4p^2k^2} \\
&\quad -\frac{q\pi^2\tanh q\pi\ \coth k\pi}{k}\frac{k^2+p^2-q^2}{(k^2+q^2-p^2)^2-4q^2k^2} \\
&\quad +\frac{2p\pi\, q\pi\ \tanh p\pi\ \tanh q\pi}{(k^2-p^2-q^2)^2-4p^2q^2}.
\end{aligned}
\tag{2.63}
$$

Integrating over $\vec{p}$ and $\vec{q}$ with $\vec{k}=\vec{p}-\vec{q}$ then gives $\mathcal{BF}-\mathcal{F}^2/2$.

Other aspects of the two-loop calculation include contracting the space-time indexes, computing the Casimir and the fermion trace. Assembling all the factors, we finally have

$$
\begin{aligned}
F^{\mathrm{B}}_{\mathrm{two-loop}} &= -g^2_{\mathrm{YM}}N^3V_3\,\mathcal{B}^2\left\{\frac{1}{8}(-24)+\frac{1}{8}(-60)+\frac{1}{4}(-48)\right. \\
&\qquad\qquad \left. +\ \frac{1}{2}\left[\frac{1}{6}(27)+\left(-\frac{1}{2}\right)+\frac{1}{2}(18)\right]\right\} \\
&= g^2_{\mathrm{YM}}N^3V_3\,16\left(\frac{T^2}{12}+\infty^2\right)^2 \\
&= g^2_{\mathrm{YM}}N^3V_3\,16\left(\frac{T^4}{144}+\frac{T^2}{6}\infty^2+\infty^4\right),
\end{aligned}
\tag{2.64}
$$

$$
\begin{aligned}
F^{\mathrm{F}}_{\mathrm{two-loop}} &= -g^2_{\mathrm{YM}}N^3V_3(\mathcal{BF}-\frac{1}{2}\mathcal{F}^2)\left[\frac{1}{2}(16+48)\right] \\
&= -g^2_{\mathrm{YM}}N^3V_3\,32\left[\left(\frac{T^2}{12}+\infty^2\right)\left(-\frac{T^2}{24}+\infty^2\right)-\frac{1}{2}\left(-\frac{T^2}{24}+\infty^2\right)^2\right] \\
&= g^2_{\mathrm{YM}}N^3V_3\,16\left(\frac{5}{4}\frac{T^4}{144}-\frac{T^2}{6}\infty^2-\infty^4\right).
\end{aligned}
\tag{2.65}
$$

Note the *exact* cancellation of the infinities between the bosonic and the fermionic contributions. Therefore, the free energy of $\mathcal{N} = 4$ $U(N)$ SYM theory at the two-loop level is given by

$$F_{\mathrm{two-loop}} = F^{\mathrm{B}}_{\mathrm{two-loop}} + F^{\mathrm{F}}_{\mathrm{two-loop}} = \frac{1}{4} g^2_{\mathrm{YM}} N^3 T^4 V_3. \tag{2.66}$$

Comparing to Eq. (2.26), we see

$$f_{\mathrm{two-loop}} = -\frac{3}{2\pi^2}\lambda. \tag{2.67}$$

So the first correction to $f(\lambda)$ at small coupling does decrease as has been conjectured before. However, this behavior is quite misleading as higher order corrections can reverse the direction.

As an aside, we mention the above two-loop calculation can be generalized to all SYM theories in four dimensions. The free energy at $\lambda \ll 1$ is

$$F = -\frac{\pi^2}{6} N^2 T^4 V_3 \left(\frac{1}{4}\mathcal{N} - \frac{3\lambda}{32\pi^2}\mathcal{N}^2 + \cdots \right), \tag{2.68}$$

where $\mathcal{N} = 1, 2, 4$ depending on the amount of supersymmetry of the theory. This general result was obtained by the author about one month prior to the appearance of [26] and is not contained there. The $\mathcal{O}(\mathcal{N})$ term is obvious since at one-loop there is no interaction and it merely counts all the degrees of freedom. We suspect the $\mathcal{O}(\mathcal{N}^2)$ term might not be a numerical coincidence. Because $\mathcal{N} = 4$ SYM theory can be viewed as a $\mathcal{N} = 2$ SYM plus a hypermultiplet, or as a $\mathcal{N} = 1$ SYM plus three chiral multiplets, it is conceivable that supersymmetry can conspire to contribute such a nice form.

2.3 Higher Order Corrections

Based on the two-loop calculation, we can update the previous result of the free energy Eq. (2.26):

$$F = -\frac{\pi^2}{6} f(\lambda) N^2 T^4 V_3,$$

where

$$\begin{aligned} f(\lambda \ll 1) &= 1 - \frac{3}{2\pi^2}\lambda + \cdots && \text{at weak coupling,} \\ f(\lambda \gg 1) &= \frac{3}{4} + \frac{45}{32}\zeta(3)(2\lambda)^{-3/2} + \cdots && \text{at strong coupling.} \end{aligned}$$

It has been argued in [42] that the general form of the λ expansion in the weak and strong coupling regimes should look like

$$\begin{aligned} f(\lambda \ll 1) &= \sum_{n\geq 0} a_n \lambda^n + \sum_{n\geq 0} b_n \lambda^{\frac{3}{2}+n} && \text{at weak coupling,} \\ f(\lambda \gg 1) &= \frac{3}{4} + \sum_{n\geq 0} c_n \lambda^{-\frac{3}{2}-n} + \sum_{n\geq 0} d_n \lambda^{-2-n} && \text{at strong coupling.} \end{aligned}$$

The a_n terms are expected from the usual loop expansion. Written in the double line notation, each closed loop carries a N factor, which combines with $g_{\rm YM}^2$ from the vertices to form λ. The b_n terms are a new feature at finite temperature. Because of thermal fluctuations, gluons get an electric mass $m_{\rm el} \propto \sqrt{\lambda}T$ at one-loop level [43]. This color screening makes heavy quarks deconfine at high temperature in QCD. The self energy of gluons and scalars contributes to the free energy via the so-called ring diagrams and renders the weak coupling expansion nonanalytic in λ. So $\lambda = 0$ becomes a branch point in the complex λ plane. On the other hand, the large λ expansion can be obtained by analyzing the closed string Virasoro-Shapiro amplitude. Expanding in α', we can get the corresponding higher derivative corrections to the Einstein gravity. This is then translated into the $\lambda^{-1/2}$ expansion via the AdS/CFT correspondence (see Table 1.1). In fact, the c_n and d_n terms come from the α'^{3+2n} and α'^{4+2n} corrections respectively. We see $\lambda = \infty$ is a second branch point.

Now the question is whether there are other singularities on the positive real axis in the λ plane. If they do exist, then there is a phase transition at some finite λ and $f(\lambda)$ can not be smoothly continued from zero to infinity. In [42], it was argued by using Mellin transform that such continuation is impossible. It would be helpful to look at more sub-leading corrections to get a clue to the validity of this argument. On the supergravity side, it is really hard to push the calculation further because currently there are no higher derivative corrections to the supergravity action available other than the $\alpha'^3 R^4$ term. The finite-temperature calculation has been improved to include the b_0 term [44], so we have

$$f(\lambda \ll 1) = 1 - \frac{3}{2\pi^2}\lambda + \frac{3+\sqrt{2}}{\pi^3}\lambda^{\frac{3}{2}} + \cdots . \tag{2.69}$$

Accordingly, Fig. 2.2 should be updated. Then it seems at this level the singularity may well exist. However, an improvement on the fixed-order perturbative calculation by Padé approximant can reverse the direction of the curve in Fig. 2.5 [44]. Furthermore, there will be new corrections like $\mathcal{O}(\lambda \ln \lambda)$ and the perturbation theory actually breaks down at order $\mathcal{O}(\lambda^3)$ [45]. This is due to a new infrared divergence associated with the exchange of magnetostatic

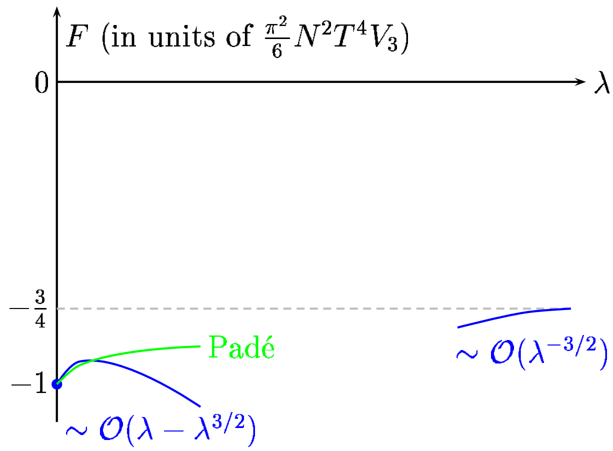

Figure 2.5: The updated free energy of $\mathcal{N} = 4$ $U(N)$ SYM theory as a function of the 't Hooft coupling λ, where the green curve is the Padé approximant.

gluons, which get a mass $m_{\text{mag}} \propto \lambda T$ at two-loop level. All diagrams above four-loop will contribute to the $\mathcal{O}(\lambda^3)$ term, so it is impractical to sum all these diagrams. The higher order terms beyond $\mathcal{O}(\lambda^3)$ can only be obtained by some nonperturbative method. Therefore, the question about the singularity and phase transition still remains unsolved to this day.

Chapter 3

Interacting Dipoles from Matrix Formulation of Noncommutative Gauge Theories

3.1 Introduction

Noncommutative quantum field theories have been extensively studied in the past few years. The motivation to study these systems stems from the fact that noncommutative gauge theories arise naturally from string theory through various decoupling limits [4][5]. However, the infrared behavior of noncommutative quantum field theories remains poorly understood due to a UV-IR connection in which the IR dynamics is not decoupled from the UV. In particular, the UV region of loop integration in Feynman diagrams leads to non-analytic behavior in external momenta indicative of novel IR dynamics [7][46].

Recently, the insight of [47] and [48] as well as [49][50] has shed some light on the interpretation of the leading IR singularities that occur in non-supersymmetric noncommutative theories. The authors of [47][48], working in the matrix formulation of noncommutative gauge theory, were able to match the leading one-loop IR singularity with an instantaneous two-body interaction between gauge invariant operators. Moreover, their results had a natural interpretation in terms of string and brane degrees of freedom that appear in matrix theory.

Actually, in the decoupling limit of open string theory in which noncommutative Yang-Mills (NCYM) emerges as the low energy effective theory, the remaining degrees of freedom are known to be extended objects [5]. In particular, the quanta can be thought of as dipoles with a transverse size proportional to their center of mass momentum. In fact, this is the origin of UV-IR mixing: high momentum dipoles grow long in spatial extent. We, therefore, intuitively expect instantaneous interactions between distant points mediated by long dipoles. However, in the conventional star product approach to noncommutative field theory, the intrinsic dipole structure of the elementary quanta is far from clear, although some suggestive results have been obtained [49].

Perhaps the most important lesson gleaned from [47][48] is that the matrix formulation is the most natural framework in which to study noncommutative gauge theory. While [48] did not demonstrate the intrinsic dipole structure of NCYM in the sense of [5], it did show that the noncommutative gauge invariance is manifest, which leads to immense simplification at the technical level. Moreover, since matrix models naturally describe extended objects, one might hope that the intrinsic dipole structure could be made manifest as well, similar to the spirit of the bi-local representation discussed in [47]. Surely, this would lead to great conceptual clarity regarding the physics of NCYM. With this in mind, we seek to study noncommutative gauge theory in the matrix formulation in order to develop a better intuition for the physics of dipole theories and the corresponding UV-IR connection.

However, there are some technical as well as conceptual obstacles to be overcome. At the technical level, problems typically arise because conventional field theory techniques often lead to ambiguous IR behavior, essentially because, in the light of noncommutativity, UV and IR are no longer synonymous with short distance and long distance, respectively. Therefore, in order to proceed, we will have to develop new calculational tools which will allow us to calculate, in a straight forward fashion, terms in the quantum effective action. We are then left to interpret the results. The conceptual challenge is then to understand the matrix calculation in conventional field theory terms, in addition to identifying the effects of the fundamental dipole structure and the corresponding UV-IR mixing.

In order to develop an intuition for the IR behavior of noncommutative gauge theory, we calculate the Wilsonian quantum effective action for the gauge field, in the matrix approach. After deriving the matrix propagator, we proceed with perturbative calculations, which yield interaction terms suggestive of dipole degrees of freedom. As expected, these dipoles have a length proportional to their center of mass momentum, and therefore, integrating out UV dipoles will lead to instantaneous long distance interactions. In fact, the leading long distance interactions, that dominate in the IR, will be due to the virtual UV dipoles. We are finally left with a very clear and intuitive picture of the dynamics resulting from dipole degrees of freedom and UV-IR mixing, which is reminiscent of the bi-local field representation discussed in [47].

We will review the matrix formulation of noncommutative gauge theories first, and then the background field gauge fixing which we employ in later sections in order to calculate the quantum effective action.

3.2 Matrix Formulation of NCYM

Consider the following Lagrangian describing a form of $U(M)$ symmetric matrix quantum mechanics

$$L = \mathrm{Tr}\left\{\frac{1}{2}(\dot{X}^i - i[A_0, X^i])^2 + \frac{1}{4}[X^i, X^j][X^i, X^j] + \cdots\right\} \tag{3.1}$$

where (A_0, X^i) are $M \times M$ hermitian matrices transforming in the vector representation of $SO(2p, 1)$ and the adjoint representation of $U(M)$. The $\cdots$ represent other fields such as the fermions in the supersymmetric theory. However, in the following we will discuss only the treatment of the bosonic fields, the generalization to fermions being obvious.

In the $M \to \infty$ limit, we can consider the classical ground state given by $X^i = \hat{x}^i \otimes \mathbb{1}_{N\times N}$ and $A_0 = 0$ where $\hat{x}^i$ are time-independent hermitian matrices satisfying the algebra of the noncommuting $2p$-plane

$$[\hat{x}^i, \hat{x}^j] = i\theta^{ij}\mathbb{1}. \tag{3.2}$$

θ^{ij} is a real constant anti-symmetric tensor of $SO(2p)$. Following [51], we expand in fluctuations about this background $X^i = \hat{x}^i \otimes \mathbb{1}_{N\times N} + \theta^{ij}A_j(\hat{x})$ and

$A_0 = A_0(\hat{x})$. The resulting action describes NCYM

$$L = \int d^{2p}x \, \mathrm{tr}_N \left\{ \frac{1}{2} G^{ij} F_{0i}(x) F_{0j}(x) \right.$$
$$\left. - \frac{1}{4} G^{ij} G^{kl} \left[F_{ik}(x) - \theta^{-1}{}_{ik} \right] \left[F_{jl}(x) - \theta^{-1}{}_{jl} \right] + \cdots \right\} \tag{3.3}$$

where $F_{\mu\nu}(x) = \partial_\mu A_\nu(x) - \partial_\nu A_\mu(x) - iA_\mu(x) * A_\nu(x) + iA_\nu(x) * A_\mu(x)$ is the noncommutative field strength, and $G^{ij} = \theta^{ik}\theta^{kj}$ is the inverse spatial metric. In deriving the NCYM theory, we have used the standard map between ordinary coordinates and noncommuting matrix coordinates [52]

$$A(x) * B(x) \quad \longleftrightarrow \quad A(\hat{x}) B(\hat{x}),$$
$$\int d^{2p}x \, \mathrm{tr}_N \left[A(x) * B(x) \right] \quad \longleftrightarrow \quad \mathrm{Tr} \left[A(\hat{x}) B(\hat{x}) \right]. \tag{3.4}$$

Note that, for notational simplicity, we have set $(2\pi)^{2p} \det(\theta) = 1$.

Thus, $2p + 1$ dimensional NCYM with a constant background field strength can be described by $0 + 1$ dimensional matrix quantum mechanics. From this point on, we will work almost exclusively in the matrix picture; however, we will eventually arrive at an interpretation of the dynamics in $2p + 1$ dimensions.

Ultimately, we will be interested in the IR behavior of the noncommutative gauge field in the quantum theory. We can systematically compute the quantum effective action by expanding the fields $A_0 = B_0 + A$ and $X^i = B^i + Y^i$ where B_0 and B^i are background fields satisfying the equations of motion, while A and Y^i are fluctuating fields to be integrated out. For our purpose, we will specialize to backgrounds of the form $B_0 = 0$ and $B^i = \hat{x}^i \otimes \mathbb{1}_{N\times N} + \theta^{ij} A_j(\hat{x})$.

In order to define the functional integral over A and Y^i, we must gauge fix the Lagrangian. This can be accomplished by adding both a gauge fixing and a ghost term to the action

$$\begin{aligned}
L_{\text{gf}} &= \text{Tr}\left\{-\frac{1}{2}\left(-\dot{A} - i[B^i, Y^i]\right)^2\right\}, \\
L_{\text{gh}} &= \text{Tr}\left\{\dot{\bar{c}}\left(\dot{c} - i[A, c]\right) + [B^i, \bar{c}][X^i, c]\right\}.
\end{aligned} \tag{3.5}$$

Upon expanding in fluctuations, the action takes the form $L = L_0 + L_2 + L_3 + L_4$ where

$$\begin{aligned}
L_0 &= \text{Tr}\left\{\frac{1}{2}\dot{B}^{i2} + \frac{1}{4}[B^i, B^j][B^i, B^j]\right\}, \\
L_2 &= \text{Tr}\left\{\frac{1}{2}\dot{Y}^{j2} + \frac{1}{2}[B^i, Y^j]^2 - \frac{1}{2}\dot{A}^2 - \frac{1}{2}[B^i, A]^2 + \dot{\bar{c}}\dot{c}\right. \\
&\qquad \left. + [B^i, \bar{c}][B^i, c] + [B^i, B^j][Y^i, Y^j] - 2i\dot{B}^i[A, Y^i]\right\}, \\
L_3 &= \text{Tr}\left\{[B^i, A][A, Y^i] + [B^i, Y^j][Y^i, Y^j] + [B^i, \bar{c}][Y^i, c]\right. \\
&\qquad \left. - i\dot{Y}^i[A, Y^i] - i\dot{\bar{c}}[A, c]\right\}, \\
L_4 &= \text{Tr}\left\{\frac{1}{4}[Y^i, Y^j][Y^i, Y^j] - \frac{1}{2}[A, Y^i]^2\right\}.
\end{aligned} \tag{3.6}$$

From L_2, we see that all of the fluctuating fields have similar quadratic terms up to terms proportional to $i\dot{B}^i$ and $[B^i, B^j]$. If we write the background field in terms of the noncommutative gauge field, $B^i = \hat{x}^i \otimes \mathbb{1}_{N\times N} + \theta^{ij}A_j(\hat{x})$, we find that

$$i\dot{B}^i = i\theta^{ij}F_{0j} \qquad [B^i, B^j] = i\theta^{ik}\theta^{lj}(F_{kl} - \theta^{-1}{}_{kl}). \tag{3.7}$$

Thus, these terms are proportional to the background gauge field strength. As is well known, the background field dependence of the terms quadratic in the fluctuating fields can either be treated exactly or perturbatively, depending on the definition of the propagator. In our calculation, it will be most convenient to treat the field strength terms (3.7) perturbatively, while absorbing the remaining background dependence into the propagator. From a physical standpoint, this choice corresponds to a derivative expansion of the background field. However, we will consider only the leading order long distance interactions, in which case commutator terms will be suppressed.

3.3 Matrix Propagator

As discussed above, all of the fluctuating fields, $\Phi = (Y^i, A, \bar{c}, c)$ corresponding to gauge field degrees of freedom, have similar quadratic terms of the form

$$\mathrm{Tr}\left\{\frac{1}{2}\dot{\Phi}^2 + \frac{1}{2}[B^i, \Phi]^2\right\}. \tag{3.8}$$

In terms of indices living in the fundamental and anti-fundamental representations of $U(\infty)$, the adjoint matrix $\Phi = \Phi_b{}^a$. In matrix notation, the quadratic term becomes

$$\begin{aligned}&\frac{1}{2}\Phi_b{}^a\left(-\delta_c{}^b\delta_a{}^d\frac{d^2}{dt^2} - B^i{}_e{}^b B^i{}_c{}^e\delta_a{}^d\right.\\ &\qquad\qquad \left.-\delta_c{}^b B^i{}_e{}^d B^i{}_a{}^e + 2B^i{}_c{}^b B^i{}_a{}^d\right)\Phi_d{}^c\\ &= \frac{1}{2}\Phi^T\left[-\mathbb{1}\otimes\mathbb{1}\frac{d^2}{dt^2} - (B^i\otimes\mathbb{1} - \mathbb{1}\otimes B^i)^2\right]\Phi.\end{aligned} \tag{3.9}$$

In the Wilsonian scheme, we are only interested in integrating out virtual states with frequencies $\omega \gg 1/T$, T being the time scale set by the background. For these high frequency modes, the back-reaction coming from the background time dependence is a subleading effect. Therefore, the matrix propagator for virtual states with frequencies above a Wilsonian cutoff, $\Lambda \gg 1/T$, can be expressed in the following Fourier integral form

$$G(t-t') = \int_\Lambda \frac{d\omega}{2\pi} \frac{e^{-i\omega(t-t')}}{\omega^2 - M^2} + \cdots \tag{3.10}$$

where $M^2 = (B^i \otimes \mathbb{1} - \mathbb{1} \otimes B^i)^2$ and the $\cdots$ represent subleading terms that are suppressed by factors of $(T\Lambda)^{-1} \ll 1$. In the following, we consider only the leading order term.

To relate this $0+1$ dimensional matrix quantity to a $2p+1$ dimensional field theory quantity, we choose a convenient representation which is derived in Appendix C

$$\begin{aligned}
&\frac{1}{\omega^2 - M^2} \\
&= \int \frac{d^{2p}k}{(2\pi)^{2p}} e^{-ik\cdot(B\otimes 1 - 1\otimes B)} \int_{\theta\Lambda} d^{2p}x \frac{e^{ik\cdot x}}{\omega^2 - x^2} \\
&= \int \frac{d^{2p}k}{(2\pi)^{2p}} e^{-ik\cdot B} \otimes e^{ik\cdot B} \int_{\theta\Lambda} d^{2p}x \, e^{ik\cdot x} \widetilde{G}(\omega, \theta^{-1}x)
\end{aligned} \tag{3.11}$$

where $\widetilde{G}(\omega, p) = (\omega^2 - p_i G^{ij} p_j)^{-1}$ is the field theory momentum space propagator for a massless state. As discussed in the appendix, there is a lower cutoff applied to the integral over x such that $x > \theta\Lambda \gg \theta/L$ where L is the length scale set by the background. Putting everything together, the matrix propagator can be written in the following form

$$\begin{aligned}
G(t-t') = \int_{\theta\Lambda} d^{2p}x \int_\Lambda \frac{d\omega}{2\pi} \int \frac{d^{2p}k}{(2\pi)^{2p}} e^{-i\omega(t-t')+ik\cdot x} \\
\times \widetilde{G}(\omega, \theta^{-1}x) e^{-ik\cdot B} \otimes e^{ik\cdot B}.
\end{aligned} \tag{3.12}$$

To our knowledge, neither this representation of the propagator, nor the interpretation to follow has been previously recognized. However, our approach is reminiscent of the work in [47] regarding bi-local fields.

We can now identify the various ingredients of the $0+1$ dimensional propagator from a $2p+1$ dimensional perspective. As suggested by the notation, (ω, k) is to be identified with the spacetime energy momentum; likewise, (t, x) is the corresponding spacetime coordinate. The integral over x is then understood in terms of the nonlocality of the noncommutative field theory. Perhaps more surprising is the role played by the field theory propagator, $\widetilde{G}$. Evidently, the small k/large x region of the integral corresponding to low momentum/large distance receives contributions from *high* momentum field theory states and vice-versa. Actually, this type of behavior has a very natural interpretation in terms of the dipole degrees of freedom that we expect from the decoupling limit of open string theory in a strong NS-NS B field [5].

In the decoupling limit, the noncommutative field quanta can be thought of as dipoles with a transverse size proportional to the center of mass momentum $x^i = \theta^{ij} p_j$. It is clear that this effect is encoded in (3.12) above, since the momentum argument of the field theory propagator, $\widetilde{G}(\omega, p)$, is $p = \theta^{-1} x$. It is also clear that, due to the Fourier integral over position, these dipole states probe a transverse momentum scale $k_i \sim 1/x^i$. Combining these two relations, we arrive at $1 \sim p_i \theta^{ij} k_j$, which is a familiar result from the star product formulation [7]. In essence, this relation means that integrating out high momentum states can lead to low momentum effects, which will become more concrete in subsequent sections. Thus, it seems that (3.12) naturally describes the dipole degrees of freedom that appear in NCYM.

However, it is important to realize that this representation is only valid for dipoles of high energy and momentum. More precisely, if the background changes on time and length scales T and L, respectively, we can only integrate over frequencies $\omega \gg 1/T$ and momenta $p = \theta^{-1}x \gg 1/L$. Otherwise, the time derivatives and commutators involving the background field that were dropped in the derivation of (3.12) are no longer negligible. Therefore, the cutoff Λ is chosen such that $\Lambda \gg 1/T$ and $1/L$. In this case, the higher order commutator and time derivative corrections are suppressed by factors of $(L\Lambda)^{-1}$ and $(T\Lambda)^{-1} \ll 1$. Moreover, since the cutoff is chosen relative to the scale of the background, Λ is naturally interpreted in the Wilsonian sense.

The matrix structure of the $0+1$ dimensional propagator, which is contained entirely in the tensor product of operators of the form $\exp(ik \cdot B)$, also has an important field theory interpretation. Using the standard dictionary between noncommuting matrix coordinates and ordinary coordinates, we can identify [48]

$$e^{ik\cdot B} = e^{ik\cdot\hat{x}\otimes 1_{N\times N} + ik\cdot\theta\cdot A(\hat{x})} \longleftrightarrow P_* e^{i\int_0^1 d\sigma k\cdot\theta\cdot A(x+\sigma k\cdot\theta)} * e^{ik\cdot x} \tag{3.13}$$

where P_* denotes path ordering of the exponential using the $*$ product. This object transforms in the adjoint under gauge transformation, and in particular, the trace is gauge invariant

$$\mathrm{Tr}\left(e^{ik\cdot B}\right) \longleftrightarrow \int d^{2p}x e^{ik\cdot x} \mathrm{tr}_N \left[P_* e^{i\int_0^1 d\sigma k\cdot\theta\cdot A(x+\sigma k\cdot\theta)}\right]. \tag{3.14}$$

We immediately recognize this object as an open Wilson line . In fact, this structure was essentially guaranteed by the noncommutative gauge invariance [53][54]. In later sections, when we use the matrix propagator in perturbative calculations of the effective action, we will frequently encounter the Fourier transform of the open Wilson line above. Following [48], we define the operator

$$\rho(x) = \int \frac{d^{2p}k}{(2\pi)^{2p}} e^{ik\cdot x} \mathrm{Tr}\left(e^{-ik\cdot B}\right) . \tag{3.15}$$

Note that although $\rho(x)$ is generally a nonlocal field theory operator, for $\theta \cdot k$ sufficiently small such that (3.12) is valid, it is approximately local on length scales given by the background configuration, as can be easily seen from (3.14) and (3.15). In fact, all gauge invariant Wilson line operators, which differ only by extra operator insertions, will share this property.

The interpretation of the matrix propagator in terms of dipole degrees of freedom is made more concrete in the following section by calculating the Wilsonian quantum effective action. We will find that integrating out UV virtual states gives rise to long distance interaction terms which are naturally interpreted in the dipole context discussed above. We will also identify terms that correspond to traditional renormalization of coupling constants of the theory.

(a) Matrix theory diagram

(b) Field theory diagram

Figure 3.1: One-loop contributions in the matrix versus the star product approach: (a) single matrix diagram is manifestly gauge invariant and implicitly contains all leading background dependence; (b) gauge invariance achieved by summing over all background insertions on both the outer and inner boundaries.

3.4 One-Loop Effective Action

We begin the computation of the quantum effective action at one-loop, where the advantage of the matrix formulation becomes immediately clear. The leading one-loop contribution is manifestly gauge invariant and can be expressed in a single diagram drawn in 't Hooft double line notation as shown in Fig. 3.1(a). This is to be contrasted with the field theory star product approach in which an infinite number of diagrams of the form shown in Fig. 3.1(b) must be summed up in order to achieve gauge invariance [49][50][54].

Using our representation of the propagator (3.12), the evaluation of the matrix diagram is simple. The contraction of matrix indices, as indicated by the double line diagram, gives a double trace contribution proportional to

$$\begin{aligned}&\int \frac{d\omega}{2\pi} \mathrm{Tr} \log G(\omega) \\ &= \int d^{2p}x_1 d^{2p}x_2 \rho(x_1,t)\rho(x_2,t) \int \frac{d\omega}{2\pi} \log \widetilde{G}(\omega, \theta^{-1}x_{12}) \qquad (3.16)\end{aligned}$$

where $x_{12} = x_1 - x_2$. Moreover, the contraction of spacetime vector and spinor indices contributes a factor proportional to $N_B - N_F$ where N_B and N_F are the numbers of on shell bosonic and fermionic polarization states. Note that, although we have not discussed fermions up to now, the matrix propagator for fermionic fields can be constructed in the exact same way as for the bosonic fields. Furthermore, the integrals are always assumed to be cutoff as previously discussed.

Now let us understand the structure of (3.16) a bit more in terms of conventional field theory diagrams Fig. 3.1(b). First of all, we choose to expand $\rho(x) = \mathrm{tr}_N(\mathbb{1}) + \Delta(x)$. The significance of $\Delta(x)$ is that it contains only fluctuations around the constant background. In particular, $\Delta(x)$ vanishes for trivial configurations gauge equivalent to $A_i(x) = 0$, which can be seen easily from the formulas (3.14) and (3.15). Therefore, the field theory interpretation of $\Delta(x)$ is that it represents the gauge invariant contribution from the insertions of the background gauge field into either the outer or inner boundary of the loop. On the other hand, the constant term of $\rho(x)$ is gauge field independent, and therefore, must descend from field theory diagrams with no background insertions on the corresponding outer or inner boundary.

For example, we can conclude that the Δ^0 interaction involves no insertions on either the outer or the inner boundary, and therefore, comes from field theory vacuum diagrams. Using the same reasoning, we find that the Δ^1 interactions involve background insertions on only one boundary, and therefore, are due to planar field theory diagrams. Finally, the Δ^2 interaction involves insertions on both the outer and the inner boundary, and therefore, arises from non-planar field theory diagrams. Thus, the single matrix diagram in Fig. 3.1(a) contains contributions from both planar and non-planar field theory diagrams.

However, the matrix calculation (3.16) only reproduces the leading order terms of the expansion in external momenta, as can be verified by a direct field theory calculation [48]. The reason is that in deriving the propagator (3.12), the matrix formulation naturally leads to an expansion in commutators and time derivatives. The subleading terms, as we have seen, are suppressed by factors of $(L\Lambda)^{-1}$, $1/L$ being the scale of the external momenta and Λ the scale of the Wilsonian cutoff. Clearly, this corresponds to expanding the field theory diagrams in the external momenta since the expansion parameter is the same. Thus, as alluded to earlier, the physical nature of our approximation is that of a derivative expansion of the background. In fact, order by order, the matrix approach reproduces the momentum expansion of the field theory if higher order commutators and time derivatives are retained. However, the matrix approach is best equipped to describe long distance behavior, in which case the $(L\Lambda)^{-1}$ corrections are small and the leading order term dominates.

Back to the calculation at hand, as expected, the Δ^0 and Δ^1 interactions, corresponding to planar field theory diagrams, are divergent. It is easy to see that they are proportional to

$$\int \frac{d\omega}{2\pi} d^{2p}x_{12} \log \widetilde{G}(\omega, \theta^{-1}x_{12}) = \int \frac{d\omega d^{2p}p}{2\pi(2\pi)^{2p}} \log \widetilde{G}(\omega, p). \tag{3.17}$$

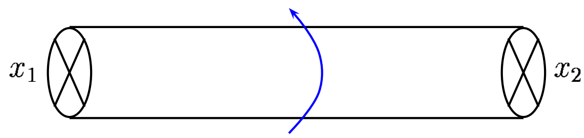

Figure 3.2: High momentum virtual dipoles grow long in the transverse direction and mediate instantaneous interactions between distant background fluctuations at x_1 and x_2.

In fact, this is nothing but the usual leading UV divergence that is familiar from field theory. It is important to note, however, that these divergent terms do not contribute to the dynamics of the background gauge field. The reason is that $\int d^{2p}x\Delta(x) = 0$, as can be seen from (3.15). The same argument is given in [48] from a different point of view. In any case, these contributions are independent of the background configuration, so we ignore them.

On the other hand, the non-planar diagrams represented by the Δ^2 interaction,

$$\int d^{2p}x_1 d^{2p}x_2 \Delta(x_1,t)\Delta(x_2,t) \int \frac{d\omega}{2\pi} \log \widetilde{G}(\omega, \theta^{-1}x_{12}), \qquad (3.18)$$

are more interesting. This term illustrates how UV dipoles can mediate long distance interactions: when the virtual dipoles in the loop have high momentum, Fig. 3.1(a) "stretches out" into a long cylinder that joins distant points x_1 and x_2. Each boundary of the cylinder contributes a trace which yields a gauge invariant Wilson line operator corresponding to the low momentum background insertions of the field theory diagrams. This process is depicted in Fig. 3.2. Thus, we can interpret the double lines in the matrix diagram as representing the physical separation of the two ends of the dipole quanta.

At this point, however, there is a technicality to be addressed. Since the leading contribution to the effective potential between $\Delta(x_1)$ and $\Delta(x_2)$ grows strong at large separation

$$\int \frac{d\omega}{2\pi} \log \widetilde{G}(\omega, \theta^{-1}x_{12}) \sim |x_1 - x_2| + \text{constant}, \tag{3.19}$$

the theory, in the presence of this term, is strongly interacting at long distances. This fact has been recognized in [48], and it was shown that these strong long distance interactions are due to the leading IR pole singularities that appear in non-supersymmetric noncommutative theories. The significance of the poles has also been discussed in [49][50]. However, we seek a weakly coupled long distance description, since otherwise, we can not treat the system perturbatively. Therefore, we demand $N_{\rm B} = N_{\rm F}$, in which case the leading interaction cancels.

We must now consider the next to leading order one-loop contribution, which has also been discussed from the star product perspective in [50]. As alluded to earlier, the precise result requires that we keep the next to leading order commutators that were dropped in the derivation of the propagator, as well as extra insertions of the background field strength coming from terms in L_2 that were also excluded from the propagator. However, power counting as well as symmetry arguments imply that the next to leading order one-loop contribution will be of the same order as Fig. 3.1(a) with two extra insertions of the field strength

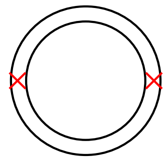 .

This contribution alone suffices to demonstrate the qualitative features of the next to leading order one-loop behavior. It has the added virtue that the calculation can be done with the propagator (3.12) because the field strength insertions are already higher order. A straight forward calculation outlined in Appendix D gives a term in the action proportional to

$$\begin{aligned}\int dt d^{2p}x_1 d^{2p}x_2 \left[\rho_{FF}(x_1,t)\rho(x_2,t) - \rho_F(x_1,t)\rho_F(x_2,t)\right] \\ \times \int \frac{d\omega}{2\pi}\widetilde{G}(\omega,\theta^{-1}x_{12})\widetilde{G}(\omega,\theta^{-1}x_{21})\end{aligned} \tag{3.20}$$

where the subscript F denotes an extra insertion of the operator $[B^i, B^j]$ into the end of the Wilson line. For example, an insertion of an arbitrary operator $\mathcal{O}$ into the end of the Wilson line gives

$$\rho_{\mathcal{O}}(x) = \int \frac{d^{2p}k}{(2\pi)^{2p}} e^{ik\cdot x}\mathrm{Tr}\left(\mathcal{O}e^{-ik\cdot B}\right). \tag{3.21}$$

It is reassuring that the second term of (3.20) is similar to the result found in [50] using field theory; however, the first term, which is of the same order, was not mentioned there. Moreover, the physical interpretation here in terms of dipoles is quite different.

At this point, we wish to make several comments. First of all, it is clear that (3.20) describes the instantaneous interaction between two points x_1 and

x_2, which is consistent with the long dipole picture depicted in Fig. 3.2. In fact, all one-loop matrix diagrams, which differ only by extra operator insertions, must have a similar double trace structure, and hence, have the physical interpretation as two-body interactions. Secondly, note that this calculation is manifestly IR safe due to the Wilsonian cutoff on frequency and separation. However, our approach is to be contrasted with [50], in which an *ad hoc* IR regulator is introduced as the smallest scale in the problem. Lastly, we can identify a term in (3.20) that leads to one-loop renormalization [46].

The renormalization comes from a UV divergence in the planar sector, corresponding to the constant term of ρ. The integral over position then factorizes into

$$\begin{aligned} & \int dt d^{2p} x_1 \rho_{FF}(x_1,t) \int \frac{d\omega}{2\pi} d^{2p} x_{12} \widetilde{G}(\omega, \theta^{-1} x_{12})^2 \\ = & \int dt \mathrm{Tr} \left\{ [B^i, B^j]^2 \right\} \int \frac{d\omega d^{2p} p}{2\pi (2\pi)^{2p}} \widetilde{G}(\omega, p)^2 . \end{aligned} \tag{3.22}$$

This quantity is easily recognized as the familiar one-loop contribution to the renormalization of the operator $\mathrm{Tr}[B^i, B^j]^2$. Although a systematic treatment of renormalization is beyond the scope of this work, it is clear from this example that UV dipoles in planar diagrams can lead to conventional renormalization of the theory.

The most interesting effect, however, is the long range interaction arising from the UV finite non-planar diagrams. We have seen that these terms come from high momentum dipoles that grow long in accordance with the UV-IR connection. Nonetheless, the analysis has been restricted to one-loop order.

In the next section, we consider some two loop contributions, which serve to illustrate some of the general features of higher order quantum corrections.

3.5 Higher Order Quantum Corrections

In the analysis of the last section, we found that one-loop matrix diagrams naturally lead to double trace operators in the effective action, which had the physical interpretation of instantaneous two-body interactions that were mediated by long dipoles. In this section, we will study some higher order loop effects. It's not hard to see that these diagrams will involve more traces and will, therefore, lead to instantaneous multi-body interactions. However generically, UV divergences also appear, which can lead to strong quantum corrections.

A simple example that illustrates some of the features of higher order corrections is the analysis of the two-loop diagrams that come from treating the quartic interactions to first order in perturbation theory

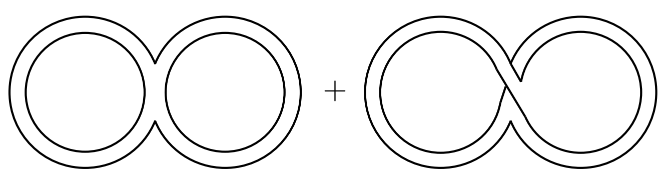

As discussed in Appendix E, the non-planar matrix diagram corresponds to field theory diagrams with the two loops linked in a non-planar fashion; however, its contribution to the Wilsonian integration is negligible. Keeping only the contribution from the planar matrix diagram, we arrive at the result derived in the appendix

$$\begin{aligned}
&\int d^{2p}x_1 d^{2p}x_2 d^{2p}x_3 \rho(x_1,t)\rho(x_2,t)\rho(x_3,t)\int \frac{d\omega_1}{2\pi}\frac{d\omega_2}{2\pi} \\
&\qquad \times \widetilde{G}(\omega_1,\theta^{-1}x_{13})\widetilde{G}(\omega_2,\theta^{-1}x_{23}) \\
\sim &\int d^{2p}x_1 d^{2p}x_2 d^{2p}x_3 \rho(x_1,t)\rho(x_2,t)\rho(x_3,t)\frac{1}{|x_1-x_3|}\frac{1}{|x_2-x_3|}. \qquad (3.23)
\end{aligned}$$

Using the same splitting scheme $\rho(x) = \mathrm{tr}_N(\mathbb{1}) + \Delta(x)$, we can extract the contributions from planar and non-planar field theory diagrams based on the powers of Δ. For example, the Δ^3 term, which descends from purely non-planar field theory diagrams, is UV finite and corresponds to an instantaneous three-body interaction as illustrated in Fig. 3.3(a). At large separations, the interaction strength falls off, so this term is consistent with a weakly coupled long distance description.

On the other hand, the terms with fewer than three Δ fields all have UV divergences arising from planar sub-diagrams in the field theory. First of all, note that the Δ^0 and Δ^1 terms are independent of the background field configuration, and therefore, do not contribute to the dynamics. We ignore these divergent terms. However, there are two distinct divergences in the Δ^2 terms which have non-trivial consequence. The first divergence comes from the constant term in either $\rho(x_1)$ or $\rho(x_2)$. In this case the integral factorizes into

$$\int d^{2p}x_1 d^{2p}x_3 \Delta(x_1,t)\Delta(x_3,t)\int \frac{d\omega_1}{2\pi}\widetilde{G}(\omega_1,\theta^{-1}x_{13})\int \frac{d\omega_2 d^{2p}p_2}{2\pi(2\pi)^{2p}}\widetilde{G}(\omega_2,p_2). \qquad (3.24)$$

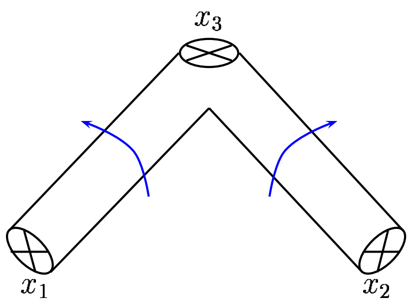

(a) Loop view

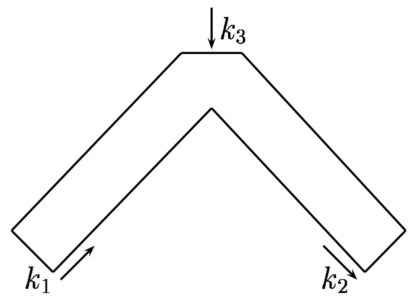

(b) Tree view

Figure 3.3: Different dipole interpretations of the first order quartic interaction: (a) shows loops of high momentum dipoles that are long in the transverse direction, as discussed in this work; (b) shows tree of low momentum dipoles that are small in the transverse direction, as discussed in [49].

This quantity is a quantum correction to the leading two-body interaction (3.18). The UV divergent loop integration can be viewed as renormalizing the coupling of this operator, which is not shown explicitly. Moreover, since the interaction strength falls with separation, this term is consistent with our perturbative analysis. However, the other divergence coming from the constant term in $\rho(x_3)$ will lead to strong interactions

$$\int d^{2p}x_1 d^{2p}x_2 \Delta(x_1,t)\Delta(x_2,t) \int \frac{d\omega_1}{2\pi} \\ \times \int \frac{d\omega_2 d^{2p}p_3}{2\pi(2\pi)^{2p}} \widetilde{G}(\omega_{21}, p_3 - \theta^{-1}x_{12})\widetilde{G}(\omega_2, p_3). \tag{3.25}$$

It is clear that this interaction grows at large separation as a power $|x_1 - x_2|^{2p-2}$ for $p > 1$ or as $\log|x_1 - x_2|$ for $p = 1$. Thus, these quantum corrections lead to strongly interacting long distance behavior.

More generally, by dimensional analysis, it is clear that strong long distance behavior can only come from UV divergences in the theory. The physical reason is that, for dipole degrees of freedom, powers of separation are the same as powers of momentum. Thus, the cancellation of strong interactions in the matrix approach is the same as cancelling UV divergences in the field theory. It is, therefore, reasonable to conjecture that, given a theory with enough supersymmetry, our perturbative analysis would exhibit weakly coupled long distance behavior, and hence, be justified. We leave this interesting and important problem for future study.

The validity of perturbation theory aside, let us focus on the robust features of our work. We have derived a matrix propagator for the quantum fields of noncommutative gauge theory that embodies the intrinsic dipole structure of the quanta as well as the UV-IR relation between the transverse size of the dipoles and their center of mass momentum. This tremendously clarified the physical effect of the quantum mechanical interactions. In particular, we found that, quite generally, the leading IR interactions are mediated by virtual UV dipoles that grow long in accordance with the UV-IR connection. This picture sheds new light on UV-IR mixing in noncommutative gauge theory, reminiscent of [47]. In fact, the intuition that we have developed seems very generic and should apply to any brand of noncommutative theory. Furthermore, in this light, the non-analytic dependence of the quantum theory on θ seems clear: in the $\theta \to 0$ limit, the quanta are no longer dipoles; therefore, the leading long distance interactions that are present for $\theta \neq 0$ abruptly disappear, drastically altering the IR behavior of the theory.

For some additional perspective, let us discuss the difference between

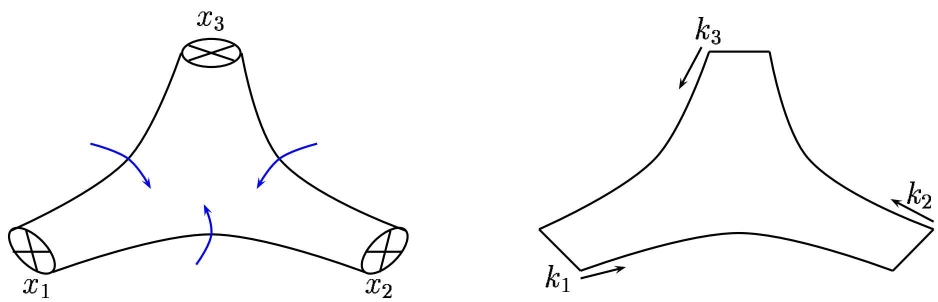

(a) Loop view (b) Tree view

Figure 3.4: Different dipole interpretations of the second order cubic interaction: (a) shows loops of high momentum dipoles that are long in the transverse direction, as discussed in this work; (b) shows tree of low momentum dipoles that are small in the transverse direction, as discussed in [49].

our work and [49]. These authors take the star product approach to studying noncommutative scalar theory and also arrive at a dipole interpretation. However, they interpret the long distance interactions as an exchange of low momentum dipole states, which is in stark contrast to the interpretation discussed here. The crucial difference is that [49] associates the k variables to dipole momentum, instead of the separation x. In particular, the Fourier coefficients $\tilde{\rho}(k)$ are interpreted as creating a dipole state of momentum k, which leads to the scenario depicted in Fig. 3.3(b). This picture seems to suggest a smooth $\theta \to 0$ limit, in which the transverse size of the dipoles goes to zero and the interaction becomes local. Apparently, this interpretation is completely different from the one discussed in our work.

Finally, for completeness, we include the contribution from the two-loop diagram arising from the second order treatment of the cubic interactions

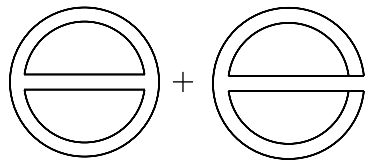

Using by now familiar techniques, we get a result proportional to

$$\int d^{2p}x_1 d^{2p}x_2 d^{2p}x_3 \rho(x_1,t)\rho(x_2,t)\rho(x_3,t) \int \frac{d\omega_1}{2\pi}\frac{d\omega_2}{2\pi}$$
$$\times \omega_1 \widetilde{G}(\omega_1, \theta^{-1}x_{12})\omega_2 \widetilde{G}(\omega_2, \theta^{-1}x_{23})\widetilde{G}(\omega_{12}, \theta^{-1}x_{31}). \tag{3.26}$$

This process is illustrated in Fig. 3.4. However, we will not pursue the analysis of this term any further since it is essentially identical to the analysis of (3.23).

Before closing this section we would like to emphasize the advantage of the matrix formulation for calculating long distance interactions. The main simplification is that the noncommutative gauge invariance is manifest, and hence, the Wilson line structure emerges automatically. Furthermore, the physical interpretation in terms of dipole degrees of freedom is clarified tremendously. However, we have only studied the leading order long distance behavior. Higher order terms in the derivative expansion must be retained in order to probe the short distance structure of the theory.

3.6 Discussion and Outlook

We have calculated the Wilsonian quantum effective action of noncommutative gauge theory in order to gain some intuition for the IR dynamics of this system. We found interaction terms suggestive of the dipole degrees of freedom that are expected from the decoupling limit of open string theory in a strong NS-NS B field. Moreover, the leading IR interactions were mediated by long UV dipoles. In fact, this is the origin of the UV-IR mixing: UV dipoles grow long and mediate long range interaction that dominate in the IR. This behavior sheds new light on the non-analytic dependence of the quantum theory on θ, which classically, is a smooth deformation.

Perhaps the most satisfying of our results was that we constructed a representation for the matrix propagator that embodies the intrinsic dipole structure of the elementary quanta of NCYM and the corresponding UV-IR connection. This approach vastly simplified calculations of the long distance interactions, as well as the physical interpretation in terms of interacting dipoles. However, our perturbative analysis is valid only when theory is weakly coupled at long distances. We argued that this is the case in supersymmetric theories, where UV quantum corrections are under control.

Finally, there remain some open questions. Most notable is that the short distance behavior is still unknown. Our analysis is insufficient to describe the quantum effects of short dipoles, which are very sensitive to the background field configuration. In this case, higher order terms in the derivative expansion must be retained. Of course, we expect some short distance corrections in the form of star products in the interaction terms; however, it would be very interesting to see some other novel effect from noncommutativity.

Appendices

Appendix A

Sommerfeld-Watson Transformation

The Sommerfeld-Watson Transformation [41] is a way to sum certain types of series via contour integration. The basic idea is to construct a complex function $f(z)$ which has these properties: it has an infinite number of poles whose residues correspond to the series; in addition, it may have some other finite number of poles; and it dies out fast enough as $z \to \infty$. Now consider the integral along the blue contour C_∞ plus all the small circles around the poles.

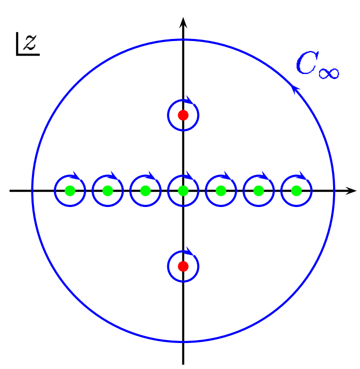

The infinite sequence of green dots denote the series and the finite number of red dots are the other poles. By construction, we have

$$0 = \oint_{C_\infty} f(z)dz - 2\pi i \sum_{\text{green}} \operatorname{Res}\left[f(z)\right] - 2\pi i \sum_{\text{red}} \operatorname{Res}\left[f(z)\right]. \tag{A.1}$$

Since the integration along C_∞ vanishes, the summation of the series is given by the residues at those extra poles

$$\sum_{\text{green}} \mathrm{Res}\,[f(z)] = -\sum_{\text{red}} \mathrm{Res}\,[f(z)]\,. \tag{A.2}$$

Applying this method to Eq. (2.52), we construct $f(z) = \cot(\pi z)/(z^2+p^2)$, which has poles at $z = n \in \mathbb{Z}$ and $z = \pm ip$. The residues are

$$\begin{aligned}
\mathrm{Res}_{z=n}\left[\frac{\cot(\pi z)}{z^2+p^2}\right] &= \frac{1}{\pi(n^2+p^2)},\\
\mathrm{Res}_{z=\pm ip}\left[\frac{\cot(\pi z)}{z^2+p^2}\right] &= \frac{\cot(\pm ip\pi)}{\pm 2ip} = -\frac{\coth(p\pi)}{2p}.
\end{aligned}$$

So we get

$$\sum_{n\in\mathbb{Z}} \frac{1}{n^2+p^2} = \frac{\pi}{p}\coth(p\pi). \tag{A.3}$$

The summation over half integers can be obtained similarly by choosing $f(z) = \tan(\pi z)/(z^2+p^2)$ and it is

$$\sum_{n\in\mathbb{Z}+\frac{1}{2}} \frac{1}{n^2+p^2} = \frac{\pi}{p}\tanh(p\pi). \tag{A.4}$$

The double-summation in Eq. (2.59) can be performed by summing over n first. The related function is

$$f(z) = \frac{\cot(\pi z)}{(z^2+p^2)\left[(z+m)^2+k^2\right]},$$

which has poles at $z = n \in \mathbb{Z}$, $z = \pm ip$ and $z = -m \pm ik$. Summing up all four residues, we have

$$
\begin{aligned}
&\sum_{n\in\mathbb{Z}} \frac{1}{(n^2+p^2)\left[(n+m)^2+k^2\right]} \\
&= \frac{\pi\coth p\pi}{p}\frac{-p^2+m^2+k^2}{(-p^2+k^2+m^2)^2+4m^2p^2} \\
&\quad+\frac{\pi\coth k\pi}{k}\frac{-k^2+m^2+p^2}{(-k^2+p^2+m^2)^2+4m^2k^2}.
\end{aligned} \tag{A.5}
$$

Then a similar treatment of m gives the result quoted in Section 2.2. All the other summations there can be computed in the same fashion.

Appendix B

Direct Calculation of the Bosonic Cross Term

After substituting $\vec{k} = \vec{p} + \vec{q}$, Eqs. (2.59) and (2.60) become

$$\sum_{n,m\in\mathbb{Z}} \frac{1}{(n^2+p^2)(m^2+q^2)[(n+m)^2+(\vec{p}+\vec{q}\,)^2]}$$
$$= \frac{\pi^2}{2p^2q^2(\cos^2\theta-1)} \left[1 + \frac{\coth p\pi\, \coth k\pi}{k}(-p - q\cos\theta) \right. \tag{B.1}$$
$$\left. + \frac{\coth q\pi\, \coth k\pi}{k}(-q - p\cos\theta) + \coth p\pi\, \coth q\pi \cos\theta\right],$$
$$\sum_{n,m\in\mathbb{Z}} \frac{n\,m}{(n^2+p^2)(m^2+q^2)[(n+m)^2+(\vec{p}+\vec{q}\,)^2]}$$
$$= \frac{\pi^2}{2p^2q^2(\cos^2\theta-1)} \left[-pq\cos\theta + \frac{\coth p\pi\, \coth k\pi}{k}\left(pq^2 + p^2q\cos\theta\right)\right.$$
$$\left. + \frac{\coth q\pi\, \coth k\pi}{k}\left(p^2q + pq^2\cos\theta\right) - pq\coth p\pi\, \coth q\pi\right], \tag{B.2}$$

where we have used $\vec{p}\cdot\vec{q} = pq\cos\theta$. So the sum of these two series is

$$\sum_{n,m\in\mathbb{Z}} \frac{\vec{p}\cdot\vec{q} + n\,m}{(n^2+p^2)(m^2+q^2)[(n+m)^2+(\vec{p}+\vec{q}\,)^2]}$$
$$= \frac{\pi^2}{2}\left(-\frac{\coth p\pi\, \coth k\pi}{pk} - \frac{\coth q\pi\, \coth k\pi}{qk} + \frac{\coth p\pi\, \coth q\pi}{pq}\right). \tag{B.3}$$

Now we can rescale the momentum $\vec{p} \to \beta\vec{p}/2\pi$ and get

$$\sum_{n,m\in\mathbb{Z}} \frac{\vec{p}\cdot\vec{q} + \omega_n\omega_m}{(\omega_n^2+\vec{p}^{\,2})(\omega_m^2+\vec{q}^{\,2})[\omega_{n+m}^2+(\vec{p}+\vec{q}\,)^2]} \tag{B.4}$$
$$= \frac{\beta^2}{8}\left(\frac{\coth\frac{1}{2}\beta p\, \coth\frac{1}{2}\beta q}{pq} - \frac{\coth\frac{1}{2}\beta p\, \coth\frac{1}{2}\beta k}{pk} - \frac{\coth\frac{1}{2}\beta q\, \coth\frac{1}{2}\beta k}{qk}\right).$$

Then Eq. (2.58) reads

$$\frac{1}{8}\int \frac{d^3p}{(2\pi)^3}\frac{d^3q}{(2\pi)^3}\left(\frac{\coth\frac{1}{2}\beta p\,\coth\frac{1}{2}\beta q}{pq}-\frac{\coth\frac{1}{2}\beta p\,\coth\frac{1}{2}\beta k}{pk}\right.$$
$$\left.-\frac{\coth\frac{1}{2}\beta q\,\coth\frac{1}{2}\beta k}{qk}\right). \tag{B.5}$$

It is easy to see that the double-integrations of the three terms are identical. For instance, in the second term, we can change the integration variable from q to k and have $d^3q = d^3k$ since $\vec{q} = \vec{k} - \vec{p}$ is just a translation; then it is the same as the first term. The net result is

$$-\frac{1}{8}\int \frac{d^3p}{(2\pi)^3}\frac{d^3q}{(2\pi)^3}\frac{\coth\frac{1}{2}\beta p\,\coth\frac{1}{2}\beta q}{pq} = -\frac{1}{2}\left(\int \frac{d^3p}{(2\pi)^3}\frac{\coth\frac{1}{2}\beta p}{2p}\right)^2. \tag{B.6}$$

From Eqs. (2.50) and (2.52), we see

$$\mathcal{B} = \int \frac{d^3p}{(2\pi)^3}\frac{\coth\frac{1}{2}\beta p}{2p}.$$

So this explicitly verifies that the bosonic cross term is equal to $-\mathcal{B}^2/2$. The fermionic cross term can be checked similarly.

Appendix C

Derivation of Matrix Propagator

In order to have a field theory interpretation of the matrix propagator, we seek a representation of the form

$$\frac{1}{\omega^2 - M^2} = \int \frac{d^{2p}k}{(2\pi)^{2p}} e^{-ik\cdot(B\otimes 1 - 1\otimes B)} \tilde{f}(k). \tag{C.1}$$

The Fourier coefficients, $\tilde{f}(k)$, can be constrained by acting with $\omega^2 - M^2$

$$\begin{aligned} 1 &= \int \frac{d^{2p}k}{(2\pi)^{2p}} (\omega^2 - M^2) e^{-ik\cdot(B\otimes 1 - 1\otimes B)} \tilde{f}(k) \\ &= \int \frac{d^{2p}k}{(2\pi)^{2p}} \left(\omega^2 + \partial_k^2\right) e^{-ik\cdot(B\otimes 1 - 1\otimes B)} \tilde{f}(k) + \cdots \end{aligned} \tag{C.2}$$

where the $\cdots$ represent commutator terms that are necessary to resolve the ordering of the noncommuting matrices, $B^i \otimes \mathbb{1} - \mathbb{1} \otimes B^i$. It is easy to see that the commutator corrections are negligible if

$$B^i \gg [k\cdot B, B^i], \left[k\cdot B, [k\cdot B, B^i]\right], \cdots \tag{C.3}$$

Using the expression for the background field, $B^i = \hat{x}^i \otimes \mathbb{1}_{N\times N} + \theta^{ij} A_j(\hat{x})$, we see that $[k\cdot B, \quad] = k\cdot\theta\cdot D$ where D_i is the gauge covariant derivative. Therefore the commutators are small if $\theta\cdot k \ll L$, L being the length scale set by the curvature of the background. Note that $L < \sqrt{\theta}$ because the NCYM dual description includes a constant background field strength of magnitude θ^{-1}.

Assuming that the commutators are negligible, we may keep only the leading term in above equation. Then, upon an integration by parts, the condition on $\tilde{f}$ becomes

$$\left(\omega^2 + \partial_k^2\right) \tilde{f}(k) = (2\pi)^{2p} \delta^{2p}(k). \tag{C.4}$$

From this equation, we arrive at the integral expression

$$\tilde{f}(k) = \int d^{2p}x \frac{e^{ik\cdot x}}{\omega^2 - x^2}. \tag{C.5}$$

Note that the consistency condition $\theta \cdot k \ll L$ is equivalent to $x \gg \theta/L$. We, therefore, apply a cutoff $x > \theta\Lambda \gg \theta/L$. Thus, up to commutator terms that are suppressed by factors of $(L\Lambda)^{-1} \ll 1$, we obtain the desired representation

$$\frac{1}{\omega^2 - M^2} = \int \frac{d^{2p}k}{(2\pi)^{2p}} e^{-ik\cdot(B\otimes 1 - 1\otimes B)} \int_{\theta\Lambda} d^{2p}x \frac{e^{ik\cdot x}}{\omega^2 - x^2}. \tag{C.6}$$

Appendix D

Next to Leading Order One-Loop Diagram

The qualitative features of the next to leading order one-loop behavior is contained in Fig. 3.1(a) with two extra insertions of the field strength. A straight forward perturbative treatment of the field strength term in L_2 gives

$$\begin{aligned}
&\int dt_1 d^{2p}x_1 dt_2 d^{2p}x_2 \int \frac{d\omega_1 d^{2p}k_1}{2\pi(2\pi)^{2p}} \frac{d\omega_2 d^{2p}k_2}{2\pi(2\pi)^{2p}} e^{-i\omega_1(t_1-t_2)+ik_1\cdot x_1} \\
&\times e^{-i\omega_2(t_2-t_1)+ik_2\cdot x_2} \widetilde{G}(\omega_1, \theta^{-1}x_1)\widetilde{G}(\omega_2, \theta^{-1}x_2) \\
&\times \left\{ \mathrm{Tr}\left([B^i, B^j](t_1)e^{ik_1\cdot B(t_1)}[B^i, B^j](t_2)e^{-ik_2\cdot B(t_2)}\right) \mathrm{Tr}\left(e^{-ik_1\cdot B(t_1)}e^{ik_2\cdot B(t_2)}\right) \right. \\
&\left. - \mathrm{Tr}\left([B^i, B^j](t_1)e^{ik_1\cdot B(t_1)}e^{-ik_2\cdot B(t_2)}\right) \mathrm{Tr}\left([B^i, B^j](t_2)e^{-ik_1\cdot B(t_1)}e^{ik_2\cdot B(t_2)}\right) \right\}.
\end{aligned} \tag{D.1}$$

Since we only integrate out virtual states with high energy and momentum, time derivatives of the background as well as higher commutator terms are further suppressed. Therefore, to lowest order, we obtain

$$\begin{aligned}
&\int dt d^{2p}x_1 d^{2p}x_2 \int \frac{d\omega}{2\pi} \frac{d^{2p}k_1}{(2\pi)^{2p}} \frac{d^{2p}k_2}{(2\pi)^{2p}} e^{ik_1\cdot x_1} e^{ik_2\cdot x_2} \widetilde{G}(\omega, \theta^{-1}x_1)\widetilde{G}(\omega, \theta^{-1}x_2) \\
&\times \left\{ \mathrm{Tr}\left([B^i, B^j](t)[B^i, B^j](t)e^{i(k_1-k_2)\cdot B(t)}\right) \mathrm{Tr}\left(e^{-i(k_1-k_2)\cdot B(t)}\right) \right. \\
&\left. - \mathrm{Tr}\left([B^i, B^j](t)e^{i(k_1-k_2)\cdot B(t)}\right) \mathrm{Tr}\left([B^i, B^j](t)e^{-i(k_1-k_2)\cdot B(t)}\right) \right\}.
\end{aligned} \tag{D.2}$$

after performing one integral over ω and one integral over t. Upon Fourier transforming to position space, we are finally left with (3.20).

Appendix E

Two-Loop Example

A straight forward evaluation of the quartic two-loop diagrams turns out to be proportional to

$$\int dt d^{2p}x_1 d^{2p}x_2 \int \frac{d\omega_1 d^{2p}k_1}{2\pi(2\pi)^{2p}} \frac{d\omega_2 d^{2p}k_2}{2\pi(2\pi)^{2p}} e^{ik_1\cdot x_1} e^{ik_2\cdot x_2}$$
$$\times \widetilde{G}(\omega_1, \theta^{-1}x_1)\widetilde{G}(\omega_2, \theta^{-1}x_2)$$
$$\times \left\{ \mathrm{Tr}\left[e^{ik_1\cdot B(t)}\right] \mathrm{Tr}\left[e^{-ik_2\cdot B(t)}\right] \mathrm{Tr}\left[e^{-ik_1\cdot B(t)} e^{ik_2\cdot B(t)}\right] \right.$$
$$\left. - \mathrm{Tr}\left[e^{ik_1\cdot B(t)} e^{ik_2\cdot B(t)} e^{-ik_1\cdot B(t)} e^{-ik_2\cdot B(t)}\right] \right\}. \tag{E.1}$$

As indicated by the double line diagrams, the triple trace term comes from the planar matrix diagram, and the single trace term comes from the non-planar matrix diagram.

To understand the meaning of the non-planar matrix diagram, consider the corresponding field theory vacuum diagram. As previously discussed, the vacuum diagrams are obtained by setting $A_i = 0$, in which case the background field $B^i = \hat{x}^i \otimes \mathbb{1}_{N\times N}$. Substituting this background field into the single trace term above, we find a result proportional to

$$\int dt d^{2p}x_1 d^{2p}x_2 \int \frac{d\omega_1 d^{2p}k_1}{2\pi(2\pi)^{2p}} \frac{d\omega_2 d^{2p}k_2}{2\pi(2\pi)^{2p}} e^{ik_1\cdot x_1} e^{ik_2\cdot x_2}$$
$$\times \widetilde{G}(\omega_1, \theta^{-1}x_1)\widetilde{G}(\omega_2, \theta^{-1}x_2) e^{ik_1\cdot\theta\cdot k_2} \mathrm{Tr}(\mathbb{1}). \tag{E.2}$$

Note that we have kept the higher order commutators, which lead to the phase factor $\exp(ik_1 \cdot \theta \cdot k_2)$, only to illustrate the qualitative nature of this contribution. Upon performing the k integrals and using the identity $\mathrm{Tr}(\mathbb{1}) = \int d^{2p}x_3 \mathrm{tr}_N(\mathbb{1})$, we get a term proportional to

$$\int dt d^{2p}x_3 \frac{d\omega_1 d^{2p}p_1}{2\pi(2\pi)^{2p}} \frac{d\omega_2 d^{2p}p_2}{2\pi(2\pi)^{2p}} e^{ip_1\cdot\theta\cdot p_2} \widetilde{G}(\omega_1, p_1)\widetilde{G}(\omega_2, p_2), \tag{E.3}$$

note that we have changed variables of integration to $p = \theta^{-1} \cdot x$. This term is easily recognized as the contribution to the effective action from the two loop non-planar field theory vacuum diagram below

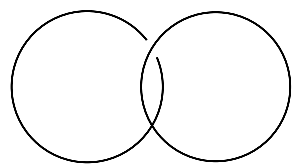

.

Thus, the non-planar matrix diagram corresponds to field theory diagrams with the loops linked in a non-planar fashion. Furthermore, it is easy to see from the single trace term in (E.1) that the effect of the background gauge field insertions is simply to include a series of higher dimensional field theory operators in the integral over x_3, and for dimensional reasons, more powers of p in the denominator. The integration over ω, p remains decoupled from the integral over x_3, though.

However, a closer look at the non-planar matrix diagram reveals that it is negligible in the domain of Wilsonian integration. In fact, the contribution is nonperturbative in our expansion parameter $(L\Lambda)^{-1}$. Essentially, the reason is that the phase factor $\exp(ip_1 \cdot \theta \cdot p_2)$ is rapidly oscillating for dipole momenta p above the Wilsonian cutoff, which gives rise to exponential suppression. To see this, consider the integration over ω, p in (E.3)

$$\begin{aligned} &\int_\Lambda \frac{d\omega_1 d^{2p}p_1}{2\pi(2\pi)^{2p}} \frac{d\omega_2 d^{2p}p_2}{2\pi(2\pi)^{2p}} e^{ip_1\cdot\theta\cdot p_2} \widetilde{G}(\omega_1, p_1)\widetilde{G}(\omega_2, p_2) \\ \sim \quad &\int_\Lambda \frac{d^{2p}p_1}{|\theta p_1|} \frac{d^{2p}p_2}{|\theta p_2|} e^{ip_1\cdot\theta\cdot p_2} \sim \Lambda^{4p-2} e^{-\theta\Lambda^2} \end{aligned} \tag{E.4}$$

where the final integration can be performed with Schwinger parameters in the stationary phase approximation. Note that $L\Lambda < \theta\Lambda$, as previously discussed. Clearly, the exponential suppression coming from the phase factor $\exp(p_1 \cdot \theta \cdot p_2)$ is universal, while the power of Λ comes from the powers of p in the integral. Thus, in the domain of Wilsonian integration, the contribution from the nonplanar matrix diagram is exponentially suppressed, and therefore, utterly negligible. In fact, the same argument implies that we can neglect all nonplanar matrix diagrams relative to the planar ones.

While nonplanar matrix diagrams do not contribute to the Wilsonian integration, they do seem to involve non-trivial short distance effects. As is well known from field theory, (E.3) is IR divergent without a cutoff [7]. Furthermore, it seems natural to attribute this to short distance effects, since the IR dipoles are small in spatial extent and only a single trace appears. Of course, it would be interesting to better understand the quantum effects of low momentum dipoles, but this is simply beyond the validity of our approximations. However, the matrix approach does seem to clarify the role of this IR singularity to the extent that it is not a long distance effect. Actually,

[47] seems to suggest that the quantum effects of low momentum states in noncommutative theories should be the same as that in ordinary theories.

Proceeding with the calculation, we keep only the triple trace term. To leading order, we neglect the commutators in (E.1), in which case we are left with

$$\int dt d^{2p}x_1 d^{2p}x_2 d^{2p}x_3 \rho(x_1,t)\rho(x_2,t)\rho(x_3,t) \int \frac{d\omega_1}{2\pi}\frac{d\omega_2}{2\pi} \times \widetilde{G}(\omega_1, \theta^{-1}x_{13})\widetilde{G}(\omega_2, \theta^{-1}x_{23}) \tag{E.5}$$

after a Fourier transformation to position space.

Bibliography

[1] T. Banks and W. Fischler, "A Model for High Energy Scattering in Quantum Gravity" [`hep-th/9906038`];

S. B. Giddings and S. Thomas, "High Energy Colliders as Black Hole Factories: The End of Short Distance Physics", *Phys. Rev.* **D65**, 056010 (2002) [`hep-ph/0106219`];

S. Dimopoulos and G. Landsberg, "Black Holes at the LHC", *Phys. Rev. Lett.* **87**, 161602 (2001) [`hep-ph/0106295`].

[2] R. Bousso, "The Holographic Principle", *Rev. Mod. Phys.* **74**, 825 (2002) [`hep-th/0203101`];

D. Bigatti and L. Susskind, "TASI Lectures on the Holographic Principle" [`hep-th/0002044`].

[3] N. Arkani-Hamed, S. Dimopoulos and G. Dvali, "The Hierarchy Problem and New Dimensions at a Millimeter", *Phys. Lett.* **B429**, 263 (1998) [`hep-ph/9803315`];

I. Antoniadis, N. Arkani-Hamed, S. Dimopoulos and G. Dvali, "New Dimensions at a Millimeter to a Fermi and Superstrings at a TeV", *Phys. Lett.* **B436**, 257 (1998) [`hep-ph/9804398`].

[4] N. Seiberg and E. Witten, "String Theory and Noncommutative Geometry", *JHEP* **09**, 032 (1999) [`hep-th/9908142`].

[5] M. M. Sheikh-Jabbari, "Open Strings in a B-field Background as Electric Dipoles", *Phys. Lett.* **B455**, 129 (1999) [hep-th/9901080];

D. Bigatti and L. Susskind, "Magnetic Fields, Branes and Noncommutative Geometry", *Phys. Rev.* **D62**, 066004 (2000) [hep-th/9908056];

Z. Yin, "A Note on Space Noncommutativity", *Phys. Lett.* **B466**, 234 (1999) [hep-th/9908152];

H. Liu and J. Michelson, "Stretched Strings in Noncommutative Field Theory", *Phys. Rev.* **D62**, 066003 (2000) [hep-th/0004013].

[6] L. Jiang and E. Nicholson, "Interacting Dipoles from Matrix Formulation of Noncommutative Gauge Theories", *Phys. Rev.* **D65**, 105020 (2002) [hep-th/0111145].

[7] S. Minwalla, M. Van Raamsdonk and N. Seiberg, "Noncommutative Perturbative Dynamics", *JHEP* **02**, 020 (2000) [hep-th/9912072].

[8] J. D. Bekenstein, "Black Holes and the Second Law", *Nuovo Cim. Lett.* **4**, 737 (1972);

J. D. Bekenstein, "Black Holes and Entropy", *Phys. Rev.* **D7**, 2333 (1973);

J. D. Bekenstein, "Generalized Second Law of Thermodynamics in Black Hole Physics", *Phys. Rev.* **D9**, 3292 (1974).

[9] S. W. Hawking, "Particle Creation by Black Holes", *Commun. Math. Phys.* **43**, 199 (1975).

[10] J. D. Bekenstein, “A Universal Upper Bound on the Entropy to Energy Ratio for Bounded Systems”, *Phys. Rev.* **D23**, 287 (1981).

[11] G. ’t Hooft, “Dimensional Reduction in Quantum Gravity” [gr-qc/9310026]; L. Susskind, “The World as a Hologram”, *J. Math. Phys.* **36**, 6377 (1995) [hep-th/9409089].

[12] W. Fischler and L. Susskind, “Holography and Cosmology” [hep-th/9806039].

[13] R. Easther and D. A. Lowe, “Holography, Cosmology and the Second Law of Thermodynamics”, *Phys. Rev. Lett.* **82**, 4967 (1999) [hep-th/9902088].

[14] D. Bak and S.-J. Rey, “Cosmic Holography”, *Class. Quant. Grav.* **17**, L83 (2000) [hep-th/9902173].

[15] R. Bousso, “A Covariant Entropy Conjecture”, *JHEP* **07**, 004 (1999) [hep-th/9905177].

[16] D. A. Lowe, “Comments on a Covariant Entropy Conjecture”, *JHEP* **10**, 026 (1999) [hep-th/9907062].

[17] R. Bousso, “The Holographic Principle for General Backgrounds” *Class. Quant. Grav.* **17**, 997 (2000) [hep-th/9911002].

[18] A. Strominger and D. Thompson, “A Quantum Bousso Bound” [hep-th/0303067].

[19] R. Bousso, “Holography in General Space-times”, *JHEP* **06**, 028 (1999) [hep-th/9906022].

[20] J. Maldacena, "The Large N Limit of Superconformal Field Theories and Supergravity", *Adv. Theor. Math. Phys.* **2**, 231 (1998) [`hep-th/9711200`];
S. S. Gubser, I. R. Klebanov and A. M. Polyakov, "Gauge Theory Correlators from Non-Critical String Theory", *Phys. Lett.* **B428**, 105 (1998) [`hep-th/9802109`];
E. Witten, "Anti De Sitter Space And Holography", *Adv. Theor. Math. Phys.* **2**, 253 (1998) [`hep-th/9802150`].

[21] O. Aharony, S. S. Gubser, J. Maldacena, H. Ooguri and Y. Oz, "Large N Field Theories, String Theory and Gravity", *Phys. Rept.* **323**, 183 (2000) [`hep-th/9905111`];
I. R. Klebanov, "TASI Lectures: Introduction to the AdS/CFT Correspondence" [`hep-th/0009139`];
E. D'Hoker and D. Z. Freedman, "Supersymmetric Gauge Theories and the AdS/CFT Correspondence" [`hep-th/0201253`].

[22] S. Kachru and E. Silverstein, "4d Conformal Field Theories and Strings on Orbifolds", *Phys. Rev. Lett.* **80**, 4855 (1998) [`hep-th/9802183`];
A. Lawrence, N. Nekrasov and C. Vafa, "On Conformal Theories in Four Dimensions", *Nucl. Phys.* **B533**, 199 (1998) [`hep-th/9803015`];
I. R. Klebanov and E. Witten, "Superconformal Field Theory on Threebranes at a Calabi-Yau Singularity", *Nucl. Phys.* **B536**, 199 (1998) [`hep-th/9807080`].

[23] J. Polchinski and M. J. Strassler, "The String Dual of a Confining Four-

Dimensional Gauge Theory" [hep-th/0003136].

[24] D. Berenstein, J. Maldacena and H. Nastase, "Strings in Flat Space and pp Waves from $\mathcal{N} = 4$ Super Yang Mills", *JHEP* **04**, 013 (2002) [hep-th/0202021].

[25] L. Jiang and A. Apte, "Two-Loop Calculation of the Free Energy of $\mathcal{N} = 4$ $D = 4$ Supersymmetric Yang-Mills Theory", *unpublished* (1998).

[26] A. Fotopoulos and T. R. Taylor, "Remarks on Two-Loop Free Energy in N=4 Supersymmetric Yang-Mills Theory at Finite Temperature", *Phys. Rev.* **D59**, 061701 (1999) [hep-th/9811224].

[27] A. W. Peet, "The Bekenstein Formula and String Theory (N-brane Theory)", *Class. Quant. Grav.* **15**, 3291 (1998) [hep-th/9712253];
D. Youm, "Black Holes and Solitons in String Theory", *Phys. Rept.* **316**, 1 (1999) [hep-th/9710046].

[28] G. 't Hooft, "The Black Hole Interpretation of String Theory", *Nucl. Phys.* **B335**, 138 (1990);
L. Susskind, "Some Speculations about Black Hole Entropy in String Theory" [hep-th/9309145].

[29] A. Strominger and C. Vafa, "Microscopic Origin of the Bekenstein-Hawking Entropy", *Phys. Lett.* **B379**, 99 (1996) [hep-th/9601029].

[30] G. T. Horowitz and A. Strominger, "Black Strings and P-branes", *Nucl. Phys.* **B360**, 197 (1991);

M. J. Duff, R. R. Khuri and J. X. Lu, "String Solitons", *Phys. Rept.* **259**, 213 (1995) [hep-th/9412184].

[31] J. Polchinski, "Dirichlet-Branes and Ramond-Ramond Charges", *Phys. Rev. Lett.* **75**, 4724 (1995) [hep-th/9510017].

[32] S. de Haro, A. Sinkovics and K. Skenderis, "On α'-corrections to D-brane solutions" [hep-th/0302136].

[33] E. Witten, "Anti-de Sitter Space, Thermal Phase Transition, And Confinement in Gauge Theories", *Adv. Theor. Math. Phys.* **2**, 505 (1998) [hep-th/9803131].

[34] G. W. Gibbons and S. W. Hawking, "Action Integrals and Partition Functions in Quantum Gravity", *Phys. Rev.* **D15**, 2752 (1977).

[35] S. S. Gubser, I. R. Klebanov and A. W. Peet, "Entropy and Temperature of Black 3-Branes", *Phys. Rev.* **D54**, 3915 (1996) [hep-th/9602135].

[36] S. S. Gubser, I. R. Klebanov and A. A. Tseytlin, "Coupling Constant Dependence in the Thermodynamics of N=4 Supersymmetric Yang-Mills Theory", *Nucl. Phys.* **B534**, 202 (1998) [hep-th/9805156].

[37] D. J. Gross and E. Witten, "Superstring Modifications of Einstein Equations", *Nucl. Phys.* **B277**, 1 (1986).

[38] J. I. Kapusta, "Finite Temperature Field Theory" (Cambridge University Press, 1989).

[39] C. W. Bernard, "Feynman Rules for Gauge Theories at Finite Temperature", *Phys. Rev.* **D9**, 3312 (1974).

[40] L. Brink, J. H. Schwarz and J. Scherk, "Supersymmetric Yang-Mills Theories", *Nucl. Phys.* **B121**, 77 (1977).

[41] A. Sommerfeld, "Partial Differential Equations in Physics", (Academic Press, 1967);
G. N. Watson, *Proc. Roy. Soc. London* **95**, 83 (1918).

[42] M. Li, "Evidence for Large N Phase Transition in N=4 Super Yang-Mills Theory at Finite Temperature", *JHEP* **03**, 004 (1999) [hep-th/9807196].

[43] D. J. Gross, R. D. Pisarski and L. G. Yaffe, "QCD and Instantons at Finite Temperature", *Rev. Mod. Phys.* **53**, 43 (1981).

[44] M. A. Vazquez-Mozo, "A Note on Supersymmetric Yang-Mills Thermodynamics", *Phys. Rev.* **D60**, 106010 (1999) [hep-th/9905030];
C. Kim and S.-J. Rey, "Thermodynamics of Large-N Super Yang-Mills Theory and AdS/CFT Correspondence", *Nucl. Phys.* **B564**, 430 (2000) [hep-th/9905205];
A. Nieto and M. H. G. Tytgat, "Effective Field Theory Approach to N=4 Supersymmetric Yang-Mills at Finite Temperature" [hep-th/9906147].

[45] A. Linde, "Phase Transitions in Gauge Theories and Cosmology", *Rep. Prog. Phys.* **42**, 389 (1979).

[46] M. Hayakawa, "Perturbative Analysis on Infrared and Ultraviolet Aspects of Noncommutative QED on R^4" [hep-th/9912167];
A. Matusis, L. Susskind and N. Toumbas, "The IR/UV Connection in the Non-communative Gauge Theories", *JHEP* **12**, 002 (2000) [hep-th/0002075];
V. V. Khoze and G. Travaglini, "Wilsonian Effective Actions and the IR/UV Mixing in Noncommutative Gauge Theories", *JHEP* **01**, 026 (2001) [hep-th/0011218];
F. R. Ruiz, "Gauge-fixing Independence of IR Divergences in Noncommutative $U(1)$, Perturbative Tachyonic Instabilities and Supersymmetry", *Phys. Lett.* **B502**, 274 (2001) [hep-th/0012171].

[47] S. Iso, H. Kawai and Y. Kitazawa, "Bi-local Fields in Noncommutative Field Theory", *Nucl. Phys.* **B576**, 375 (2000) [hep-th/0001027].

[48] M. Van Raamsdonk, "The Meaning of Infrared Singularities in Noncommutative Gauge Theories", *JHEP* **11**, 006 (2001) [hep-th/0110093].

[49] Y. Kiem, S. Lee, S.-J. Rey and H. T. Sato, "Interacting Open Wilson Lines from Noncommutative Field Theories", *Phys. Rev.* **D65**, 046003 (2002) [hep-th/0110215];
Y. Kiem, S.-J. Rey, H. T. Sato and J. T. Yee, "Open Wilson Lines and Generalized Star Product in Noncommutative Scalar Field Theories", *Phys. Rev.* **D65**, 026002 (2002) [hep-th/0106121];
Y. Kiem, S.-J. Rey, H. T. Sato and J. T. Yee, "Anatomy of One-Loop Effective Action in Noncommutative Scalar Field Theories", *Eur. Phys.*

J. **C22**, 757 (2002) [hep-th/0107106];
Y. Kiem, S. S. Kim, S.-J. Rey and H. T. Sato, "Anatomy of Two-Loop Effective Action in Noncommutative Field Theories", *Nucl. Phys.* **B641**, 256 (2002) [hep-th/0110066].

[50] A. Armoni and E. Lopez, "UV/IR Mixing via Closed Strings and Tachyonic Instabilities", *Nucl. Phys.* **B632**, 240 (2002) [hep-th/0110113].

[51] N. Seiberg, "A Note on Background Independence in Noncommutative Gauge Theories, Matrix Model, and Tachyon Condensation", *JHEP* **09**, 003 (2000) [hep-th/0008013].

[52] R. Gopakumar, S. Minwalla and A. Strominger, "Noncommutative Solitons", *JHEP* **05**, 020 (2000) [hep-th/0003160].

[53] N. Ishibashi, S. Iso, H. Kawai and Y. Kitazawa, "Wilson Loops in Noncommutative Yang-Mills", *Nucl. Phys.* **B573**, 573 (2000) [hep-th/9910004];
S.-J. Rey and R. von Unge, "S-Duality, Noncritical Open String and Noncommutative Gauge Theory", *Phys. Lett.* **B499**, 215 (2001) [hep-th/0007089];
S. Das and S.-J. Rey, "Open Wilson Lines in Noncommutative Gauge Theory and Tomography of Holographic Dual Supergravity", *Nucl. Phys.* **B590**, 453 (2000) [hep-th/0008042];
D. J. Gross, A. Hashimoto and N. Itzhaki, "Observables of Non-commutative Gauge Theories", *Adv. Theor. Math. Phys.* **4**, 893 (2000) [hep-th/0008075].

[54] H. Liu and J. Michelson, "$*$-TREK: The One-Loop N=4 Noncommutative SYM Action", *Nucl. Phys.* **B614**, 279 (2001) [hep-th/0008205];

H. Liu, "$*$-Trek II: $*_n$ Operations, Open Wilson Lines and the Seiberg-Witten Map", *Nucl. Phys.* **B614**, 305 (2001) [hep-th/0011125].

Vita

Li Jiang was born in Jiujiang, Jiangxi, China on December 14, 1972 to Jiang Xianwen and Xu Hui. He received the Bachelor of Science degree in Geophysics from the University of Science and Technology of China in 1995. He came to the United States with a Graduate School Fellowship in the Fall of 1995, studying at Brown University, Providence, Rhode Island. In August, 1996, he transferred to the University of Texas at Austin, where he began his doctoral work in the Physics Department.

Permanent address: University of Texas at Austin
Theory Group
1 University Station C1608
Austin, TX 78712-0269

This dissertation was typeset with LaTeX[†] by the author.

[†]LaTeX is a document preparation system developed by Leslie Lamport as a special version of Donald Knuth's TeX Program.